國立臺灣大學公共衛生學院環境與職業健康科學研究所

碩士論文

Institute of Environmental and Occupational Health Sciences

College of Public Health

National Taiwan University

Master's Thesis

應用質譜儀為基礎的脂質體學探討全氟辛烷磺酸暴露對人類肝癌細胞脂質影響

Lipid Alterations in HepG2 Cells Exposed to Perfluorooctanesulfonic Acid: A Mass Spectrometry-based Lipidomic Approach

賴靖丰

Ching-Feng Lai

指導教授: 林靖愉 博士

Advisor: Ching-Yu Lin, Ph.D.

中華民國 114 年 7 月

July, 2025

doi:10.6342/NTU202503955

致謝

兩年過的很快，總覺的自己離放榜那天沒有很遠。能完成碩士學業以及學術論文，需要感謝的人很多。

首先需要感謝林靖愉老師以及江素瑛老師的指導。脂質體學以及細胞毒性實驗對我而言是從未接觸的領域，很幸運在探索以及學習的過程中能有兩位老師為我指引方向。再來要感謝梁皓然、嚴子昕學長，以及張寶穗學姊在不論是論文撰寫或是學業方面皆提供非常大的協助，學長姊的幫助令我非常感激。

再來要感謝大學教授，簡伶朱老師，以及實驗室的學姊們。很感謝老師與學姊們提供優質的學習環境以及情感支持，甚是懷念。同時也要感謝親友團的支持。感謝父母讓我衣食無缺，能專心在自己的課業，並多次表達支持，非常感激。還有我的弟弟，雖然我經常晚歸，回家時你總是會跟我打招呼並出來聊個幾句，很感謝。特別感謝弈絃的支持，不論是隨時提供的情感支持，陪我度過最低朝的時候，又或是在學業上提供前人的意見，省了很多冤枉路，交往的四年總是充滿歡樂。還有在我生命中重要的狗狗們：天天、襪狗、皮蛋，以及在天上的阿福、coffee、沙沙，你們每個都是超可愛的小寶寶。最後要感謝北醫羽球隊的朋友們，讓我時不時回去蹭球場一起訓練，這兩年還能有高強度的運動實在難得，彷彿回到大學練球的時光。最後的最後，感謝口試委員們針對本研究給予的建議。

賴靖丰 謹誌 2025.08.05

doi:10.6342/NTU202503955

摘要

全氟與多氟烷基物質（per- and polyfluoroalkyl substances; PFAS）是一類廣泛應用於產品中的化學物質。其中，全氟辛烷磺酸（perfluorooctanesulfonic acid; PFOS）是最常在人體血清與環境樣本中檢測到的化合物之一。由於其對蛋白質具有高度結合親和力，PFOS 容易在肝臟中累積。PFOS 會引發多種有害健康效應，包括干擾脂質代謝、肝臟脂肪累積，以及肝臟發炎。本研究旨在透過脂質體學方法，分析 PFOS 暴露對人類肝癌細胞株 HepG2 中含磷酸膽鹼的脂質（phosphorylcholine-containing lipids; PC-CL）的變化，以探討其可能毒性機制。

本研究分別以對照組、1/10 IC_{10}、IC_{10}與 IC_{20} PFOS 濃度處理 HepG2 細胞 48 小時。細胞收集後，脂質經由改良的 Folch 法萃取，並以超高效液相層析串聯三重四極桿質譜儀分析 HepG2 細胞的 PC-CL 組成。經圖譜處理後，透過主成分分析與偏最小平方區別分析等多變量統計方法，辨識各暴露劑量組別間脂質體的差異；同時使用 Kruskal–Wallis 檢定以篩選在不同處理組之間具顯著差異的脂質種類。

在高劑量 PFOS 暴露組中，單元與雙元不飽和二酰基 PC（DPC）下降，而多元不飽和 DPC（polyunsaturated-DPC; PUFA-DPC）上升。這些結果顯示 PFOS 可能干擾肝臟中磷脂醯膽鹼的生合成路徑，包括 CDP-膽鹼(CDP-choline)路徑與磷脂醯乙醇胺 N-甲基轉移酶(phosphatidylethanolamine N-methyltransferase; PEMT)路徑。此外，PUFA-DPC 與 P-PC 的上升可能反映細胞為了對抗 PFOS 引發的發炎與氧化壓力而產生的肝保護性反應。

doi:10.6342/NTU202503955

總結而言，本研究運用了質譜為基礎的脂質體學方法，探討 PFOS 暴露對 HepG2 細胞 PC-CL 脂質組成的影響。研究結果指出，在不引起細胞毒性的 PFOS 暴露濃度下，細胞可能透過肝保護機制來應對 PFOS 所造成的發炎與氧化壓力反應。本研究的結果展現出體外實驗在脂質體學研究中作為動物實驗替代方案的潛力，特別是在相對低劑量 PFOS 暴露的情況下。

關鍵字：全氟與多氟烷基物質、全氟辛烷磺酸、體外研究、脂質代謝、肝毒性

doi:10.6342/NTU202503955

Abstract

Per- and polyfluoroalkyl substances (PFASs) are a group of synthetic chemicals widely used in consumer products. Among them, perfluorooctanesulfonic acid (PFOS) is one of the most commonly detected compounds in human serum and environmental samples. Due to its high binding affinity to proteins, PFOS accumulates in the liver. PFOS induces several adverse health effects, including the disruption of lipid metabolism, liver steatosis, and liver inflammation. The aims of this study are to understand the possible mechanisms of PFOS-induced cytotoxicity by analyzing changes of phosphorylcholine-containing lipids (PC-CL) in human hepatoma HepG2 cells exposed to a series dose of PFOS using lipidomic approach.

HepG2 cells were treated with vehicle control, 1/10 IC_{10}, IC_{10} and IC_{20} of PFOS for 48 hours. PC-CL were extracted with modified Folch method and analyzed by ultra-performance liquid chromatography–triple quadrupole mass spectrometry. After spectral processing, multivariate analysis, including principal component analysis and partial least squares discriminant analysis, were conducted to identify different patterns of lipid across the various treatment groups. The Kruskal–Wallis test was applied to identify lipids that significantly differed among treatment groups.

The decreased levels of mono- and di-unsaturated diacyl-PC (DPC) and increased levels of polyunsaturated-DPC (PUFA-DPC) were observed in the high dose group. These findings suggest

doi:10.6342/NTU202503955

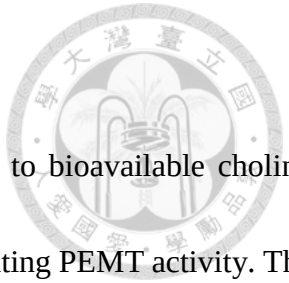

that PFOS may disrupt the hepatic PC biosynthesis pathway by binding to bioavailable choline, thereby reducing PC production via the CDP-choline pathway and upregulating PEMT activity. This compensatory mechanism may enhance PC biosynthesis through the PEMT pathway.

In conclusion, this study applied MS-based lipidomic approach to identify the changes of PC-CL profile in PFOS-treated HepG2 cells. The results suggested that at sublethal doses of PFOS, the hepatoprotective effects may occur due to the inflammation and oxidative stress caused by PFOS. The results of this study demonstrate the potential of *in vitro* models as alternatives to animal testing in lipidomic research, particularly under conditions of sublethal doses of PFOS exposure.

Keywords: per- and polyfluoroalkyl substances, perfluorooctanesulfonic acid, lipid metabolism, *in vitro* study, hepatotoxicity

doi:10.6342/NTU202503955

Content

doi:10.6342/NTU202503955

doi:10.6342/NTU202503955

List of figures

doi:10.6342/NTU202503955

List of tables

doi:10.6342/NTU202503955

Chapter 1 Introduction

1.1 Per- and polyfluoroalkyl substances PFAS

Per- and polyfluoroalkyl substances (PFAS) are a class of fluorinated chemicals characterized by the presence of at least one fully fluorinated methyl or methylene carbon atom, without any H/Cl/Br/I atom attached to it (OECD, 2021). PFAS compounds are commonly classified based on whether they are polymers or non-polymers (Dehghani et al., 2025). Non-polymer PFAS are the most frequently detected types in humans, wildlife, and various environmental media, and they tend to be more prevalent at PFAS-contaminated sites (Reiner & Place, 2015). Within the non-polymer category, PFAS can be further divided into two main groups: perfluoroalkyl substances and polyfluoroalkyl substances. Perfluoroalkyl substances are fully fluorinated alkane chains, which include perfluoroalkyl acids (PFAAs) and perfluoroalkane sulfonamides **(Figure 1)**. PFAAs represent some of the simplest PFAS structures and are highly resistant to degradation under typical environmental conditions. In contrast, many polyfluoroalkyl substances can undergo biotic or abiotic transformation, eventually producing PFAAs as end products (Gaines et al., 2023).

PFAS are known as “forever chemicals”. The strong carbon-fluorine bonds make PFAS highly resistant to chemical, biological, and thermal degradation (Evich et al., 2022; Gluge et al., 2020). PFASs possess both hydrophobic and lipophobic properties,

doi:10.6342/NTU202503955

leading to the widely production and usage in various consumer products, including food packaging, textiles, and firefighting foam, since the 1940s (Wee & Aris, 2023).

The high mobility of PFAS enables their easy movement through the environment. Short-chain PFAS (fluoroalkyl carbon number < 6) are highly soluble in water, leading to rapid transport through groundwater, while long-chain PFAS (fluoroalkyl carbon number ≥6) tend to adsorb more to soil and sediments but can still leach over time (Evich et al., 2022). The primary occupational exposure to PFAS occurs through drinking water and inhalation, while the general community is mainly exposed to PFAS through drinking water and food ingestion (Gao et al., 2015; Post et al., 2017; Wee & Aris, 2023).

PFAS compounds have been detected in human serum worldwide. Previous biomonitoring studies of human blood samples from various countries—including the United States, Colombia, Brazil, Belgium, Italy, Poland, India, Malaysia, Korea, and Japan—have shown that PFAS are detectable across different age groups in the general population. Among the PFAS compounds, perfluorooctanesulfonic acid (PFOS) was the most frequently detected and showed the highest average concentrations (Kannan et al., 2004). Moreover, PFAS are known to accumulate in the human body over time. For example, the mean half-life of PFOS in human serum is estimated to be 5.4 years (Olsen et al., 2007).

doi:10.6342/NTU202503955

Epidemiological studies have revealed that PFAS exposure may lead to several adverse health effects, including immune system dysfunction, thyroid disorders, cardiovascular disease, developmental delays, liver damage, and kidney damage (Fenton et al., 2021; Jane et al., 2022). For instance, a cross-sectional study of 200 adults from the C8 Health Study cohort, which is a PFAS-contaminated community in the USA, showed that PFAS levels were positively associated with the serum level of liver injury marker: alanine aminotransferase (ALT) and aspartate aminotransferase (AST), indicating the increased risk of liver injury induced by PFAS exposure (Darrow et al., 2016). Shankar et al. (2011) conducted a cross-sectional study analyzing data from 4,587 adults using data from National Health and Nutrition Examination Survey from 1999 to 2008. They found that concentrations of perfluorooctanoic acid (PFOA) and PFOS were negatively associated with estimated glomerular filtration rate, suggesting an increased risk of chronic kidney disease.

PFAS exposure was also found to be associated with metabolic alterations. Eriksen et al. (2013) found that total and low-density lipoprotein levels in human serum increase as human serum PFAS concentrations rise, which may lead to a higher risk of cardiovascular disease. Alderete et al. (2019) conducted a prospective longitudinal study of 40 overweight/obese Hispanic children from 8 to 14 years old in Los Angeles, USA. They found that higher plasma PFOA and perfluorohexanesulfonic acid

doi:10.6342/NTU202503955

concentrations were significantly associated with impaired glucose regulation and early risk for type 2 diabetes through metabolic disturbances.

Toxicological studies further provide insights into the biological mechanisms underlying PFAS-induced toxicity. Both *in vivo* and *in vitro* studies have linked PFAS exposure to hepatotoxicity, neurotoxicity, immunotoxicity, cardiovascular toxicity, reproductive and developmental toxicity, as well as tumor induction (Fenton et al., 2021).

Liver is considered the primary target organ of PFAS. Previous studies showed that PFAS mixtures induced liver inflammation, liver enlargement, increased liver weight, and elevated levels of injury markers and oxidative stress markers in C57BL/6J mice (Roth et al., 2021). As the liver plays important roles in lipid homeostasis, the lipid alteration is also an important effect of PFAS induced-hepatotoxicity.

Hepatic lipid metabolism is mainly regulated at gene transcription level. For instance, one of the main nuclear receptors peroxisome proliferator-activated receptor α (PPARα) involved in the regulation of hepatic lipid metabolism can be activated by PFAS (Fragki et al., 2021). Due to their structural resemblance to endogenous fatty acids, certain PFAS such as PFOS and PFOA function as ligands for PPARα, thereby acting as agonists. Activation of PPARα induces the expression of several genes participate in lipid metabolic pathways, such as fatty acid storage, β-oxidation, and

doi:10.6342/NTU202503955

transport (Kersten & Stienstra, 2017). Toxicological studies using rodent model indicates that PFOS and PFOA exposure down-regulates hepatic production of very low-density lipoprotein triglycerides (VLDL-TG) and apolipoprotein B (apoB), thereby impairing the hepatic export of TG (van der Veen et al., 2017). Additionally, PFAS exposure enhances lipoprotein lipase-mediated lipolysis of TG-rich plasma lipoproteins, result in the accumulation of hepatic TG (Martínez-Uña et al., 2013). These disruptions suggest that PFAS-induced perturbations in lipid metabolic pathways may contribute to hepatotoxic outcomes.

1.2 Perfluorooctanesulfonic acid (PFOS)

PFOS is consisting of eight fully fluorinated carbon atoms and a hydrophilic sulfonic acid functional group **(Figure 2)**. PFOS was first manufactured in the United States in 1948. In 2001, the major manufacturer phased out PFOS production. PFOS is one of the most prevalent PFAS in the environment and living organisms, even though many countries have imposed bans on PFAS for years (Brusseau et al., 2020; Control & Prevention, 2022).

PFOS is efficiently absorbed following oral exposure, with bioavailability exceeding 90% in rodent models. Dermal contact and inhalation absorption of PFAS are relatively low compared to oral intake. For example, *in vitro* studies using human

doi:10.6342/NTU202503955

skin reported a dermal permeability coefficient for PFOA of 9.49×10^{-7} cm/h, with only about 0.05% of the administered dose penetrating the skin over 48 hours (Fasano et al., 2005). After absorption, PFOS strongly binds to serum albumin, facilitating its systemic circulation and preferential accumulation in the liver, which has been identified as a primary site of deposition in rodents, non-human primates, and humans (Jian et al., 2018). In addition to hepatic accumulation, PFOS is also distributed to the kidneys, blood serum, and to a lesser extent, the spleen and brain. PFOS is considered a terminal degradation product and is not subject to further transformation in biological systems. PFOS is resistant to enzymatic degradation, including cytochrome P450-mediated metabolism. Studies have consistently shown that PFOS does not undergo phase I or phase II metabolic biotransformation in either humans or animals (Goodrum et al., 2021). PFOS elimination occurs slowly via renal and biliary routes and demonstrates notable sex-specific differences, particularly in rats: male rats exhibit significantly slower urinary clearance than females (Pizzurro et al., 2019).

Previous epidemiological studies have linked PFOS exposure to several adverse effects on the liver. Studies conducted in Hong Kong, Sweden, and the United States have found that serum PFOS concentrations were positively associated with serum levels of ALT, AST, and gamma-glutamyl transpeptidase in elderly individuals,

doi:10.6342/NTU202503955

children, or obese participants (Jain, 2019; Salihovic et al., 2018; Stratakis et al., 2020). These biomarkers suggest that PFOS exposure may contribute to liver injury.

Previous toxicological studies on PFOS have reported multiple liver-related adverse effects in animal models. In male mice, PFOS exposure has been associated with hepatomegaly and disruptions in lipid metabolism (Wan et al., 2012). A previous study conducted by Yen et al. (2024) found that PFOS exposure in male Sprague–Dawley (SD) rats led to altered phospholipid content in multiple organs, including the liver, indicating that PFOS exposure may induce hepatotoxicity.

PFOS has also been shown to trigger inflammatory responses in male CD-1 mice via activation of the nuclear factor-κB (NF-κB) signaling pathway and increased secretion of pro-inflammatory cytokines (Butenhoff et al., 2012). In addition, PFOS has been reported to induce hepatocellular degeneration and elevate plasma membrane permeability. Furthermore, chronic PFOS exposure has been linked to the development of benign hepatic tumors in SD rats (Qin et al., 2022).

The PFOS-induced hepatotoxicity can also be observed from *in vitro* studies. For instance, HepaRG cell treated with PFOS showed increased TG levels, suggesting the onset of steatosis (Louisse et al., 2020). Treatment of HepG2 cells with PFOS resulted in increased malondialdehyde (MDA) levels, suggesting oxidative stress–mediated hepatotoxicity through the overproduction of reactive oxygen species (ROS) (Amstutz

doi:10.6342/NTU202503955

et al., 2022; Li et al., 2025). In addition, a previous study using primary hepatocytes from grass carp showed that PFOS exposure promoted the release of pro-inflammatory cytokines, indicating the induction of an inflammatory response.

The choice of *in vitro* liver model is critical to accurately reflect the PFOS-induced toxicity. HepG2 cells are easy to culture, rapidly proliferate, and are cost-effective, making them ideal for high-throughput screening. Moreover, their clonal origin ensures consistent genetic background, which contributes to stable and reproducible results across experiments. However, HepG2 cells exhibit lower enzyme activity compared to HepaRG cells and primary human hepatocytes, especially the cytochrome P450 enzyme, which may restrict their ability to fully reflect PFOS-induced metabolic disturbances. HepaRG cells offer higher CYP expression and more closely mimic primary hepatocyte functions. However, HepaRG cells require long differentiation periods, more complex culture conditions, and higher operational costs. Primary human hepatocytes are considered highly representative of *in vivo* liver metabolism and transport processes. However, their utility is limited by significant donor-to-donor heterogeneity, limited tissue supply, and rapid loss of metabolic competence during culture **(Table 1)** (Wilkening et al., 2003).

doi:10.6342/NTU202503955

1.3 Possible mechanism of PFOS-induced hepatotoxicity

The mechanisms of PFAS-induced hepatotoxicity can be investigated through the use of *in vitro* models. For instance, Luo et al. (2024) examined PFAS-induced liver steatosis using high-throughput phenotypic profiling and transcriptomic data from PFAS-treated HepG2 cells. They found that PFAS exposure led to mitochondrial damage and the activation of lipid metabolism-related genes, which were associated with the development of liver steatosis. Similarly, Li et al. (2025) examined effects of several PFAS species on HepG2 cells by employing an MS-based metabolomic approach alongside measurements of oxidative stress biomarkers and the expression levels of genes involved in lipid transport, synthesis, and oxidation. These *in vitro* studies indicated that PFAS exposure may alter hepatic lipid content, upregulate lipid metabolism-related genes, and increase oxidative stress.

In addition, PFOS-induced hepatotoxicity may be through activation of hepatocyte inflammation. Previous studies on PFOS-induced hepatotoxicity have showed increased hepatic levels of proinflammatory cytokines, including IL-1β, TNF-α, and IL-6 in zebrafish and wild-type C57BL/6J mice (Guo et al., 2019; Wang et al., 2021). These findings suggest that PFOS may induce hepatotoxicity through the activation of signaling pathways related to inflammatory responses.

doi:10.6342/NTU202503955

PFOS exposure may also induce hepatotoxicity through oxidative stress. PFOS may enhance the formation of ROS, leading to endoplasmic reticulum (ER) stress (Wang et al., 2020) and lipid peroxidation by attacking unsaturated fatty acids. Moreover, the excessive ROS accumulation compromises hepatic cell membrane integrity by increasing oxidative damage, ultimately disrupting membrane stability and permeability (Zhu et al., 2022).

Previous toxicological studies revealed that PFOS exposure reduced the protein levels of nuclear factor erythroid 2-related factor 2 (Nrf2), which is a key transcription factor that protects cells from oxidative stress by upregulating genes involved in antioxidant defense and detoxification in male SD rats (Lv et al., 2013). Wan et al. (2016) also found that PFOS resulted in lower protein expression of Nrf2 and reduced protein level of NAD(P)H:quinone oxidoreductase in mice. These findings suggested that PFOS may induced hepatotoxicity through the inhibition of oxidative stress-related signaling pathways.

1.4 Lipidomics

Metabolomics is the study of the metabolome, which consists of downstream products from various biological processes. Metabolomics provide integrative insights into cellular function and reveal information that other “omics” approaches cannot

doi:10.6342/NTU202503955

obtain. By utilizing high-throughput techniques, “omic” studies facilitate a comprehensive and systematic understanding of various biological molecules. (Villas-Boas et al., 2007).

Lipidomics is a subfield of metabolomics that focuses on the study of lipids (Fiehn, 2001). Lipids are crucial compounds in the cell and serve several functions. For example, lipid act as structural components of cell membranes, participate in signaling pathways, and serve as energy storage sources (Fahy et al., 2011). Lipidomic analysis has broad applications across multiple disciplines, such as exposure science, toxicology, disease mechanism research, and biomarker discovery (Masoodi et al., 2021). By identifying lipid alterations across different lipid classes, lipidomics provides valuable insights into the health effects of environmental or chemical stressors by examining lipid alterations in biological systems (Wang et al., 2019). Lipidomics also facilitates a better understanding of disease mechanisms and supports the discovery of potential biomarkers for early diagnosis and therapeutic targets (Khanna et al., 2022).

Based on the LIPID MAPS Structure Database classification (Sud et al., 2007), lipids can be categorized into several classes, including fatty acyls (FA), sterol lipids (ST), glycerolipids (GL), sphingolipids (SP), glycerophospholipids (GP), prenol lipids, saccharolipids, and polyketides. Among these, FA, ST, GL, SP, and GP are common lipids within the mammalian cell and serve distinct roles in various biological functions.

doi:10.6342/NTU202503955

FAs act as energy sources and signaling molecules. Excessive intake of FAs is linked to obesity and metabolic disorders (Maximino et al., 2015). STs, such as cholesterol, serve as precursors for steroid hormones and bile acids; however, excess cholesterol contributes to liver inflammation and non-alcoholic fatty liver disease (NAFLD) (Malhotra et al., 2020). GLs, including diacylglycerols and triacylglycerols, primarily function as energy storage molecules but are also associated with metabolic and neurodegenerative diseases (Prentki & Madiraju, 2008). SPs, such as sphingomyelin (SM) and gangliosides, are essential for neural structure and signaling; altered SP levels are linked to disorders such as Alzheimer's disease and stroke (Saher et al., 2005). GPs, such as phosphatidylcholine (PC), are major components of cell membranes, maintaining membrane integrity and function (van der Veen et al., 2017).

Nuclear magnetic resonance (NMR) and mass spectrometry (MS) are two techniques widely used in the field of metabolomics and lipidomics. MS offers higher sensitivity and selectivity compare to NMR, and allows rapid detection of compounds based on their exact mass and fragmentation patterns. The precise molecular weight determination, making it ideal for detecting and quantifying lipids (Gathungu et al., 2020). The MS spectra generate molecular fingerprint of biological samples, providing both structural and quantitative information for biological studies (Villas-Boas et al., 2007).

doi:10.6342/NTU202503955

1.5 Application of focus lipidomic approach to phosphorylcholine-containing lipids profiling in hepatotoxicity study

Phosphorylcholine-containing lipids (PC-CL), including PCs and SMs **(Figure 3)** refer to lipids that possess a phosphorylcholine moiety as their polar head group. PC are classified into lyso-phosphatidylcholines (LPCs), diacyl-phosphatidylcholines (DPCs), O-alkyl-acyl- phosphatidylcholines (O-PCs), and O-alkenyl-acyl-phosphatidylcholines (P-PCs) **(Figure 4)**. The structure of SMs consists of a sphingosine backbone, a fatty acid chain, and a phosphocholine group as its polar head (Fahy et al., 2005).

PCs and SMs serve several important functions in the cells, including being a structural component of cell membranes, maintaining membrane integrity and fluidity. In addition, PCs and SMs are involved in cellular signaling, inflammation, and apoptosis (Akin et al., 2007). In hepatocytes, PC is crucial for VLDL assembly and the stabilization of apoB, thereby facilitating lipid export from the liver (Yao & Vance, 1988). Additionally, PC shows anti-inflammatory and antioxidant properties, especially those species enriched in polyunsaturated fatty acids (Akin et al., 2007).

Recently, the analysis of PC-CL species has emerged as a valuable tool to understand possible mechanisms of adverse health effects. For instance, Ming et al.

doi:10.6342/NTU202503955

(2017) observed that acetaminophen caused significant alterations in the hepatic lipid profile, including a notable increase in several PC species in mice. Similarly, Ling et al. (2014) reported an elevation of DPCs in the liver lipidome of male mice following naphthalene exposure, suggesting membrane damage induced by naphthalene. Yen et al. (2024) found that PFOS exposure led to significant changes in the liver lipidome, including alterations in LPCs, DPCs, and ether-linked PCs in male SD rats. These changes may be associated with PFOS-induced membrane dysfunction and oxidative stress.

Previous studies suggested that alterations in different PC-CL species may result in distinct biological consequences, highlighting the potential of PC-CL profiling not only as a tool for mechanistic studies but also for biomarker discovery in toxicological and health-related studies.

1.6 Challenge in PFAS induced-hepatotoxicity studies

Despite growing global governmental awareness of PFAS toxicity, only a few PFAS compounds have been well studied. The liver is the primary target organ of PFAS toxicity (Chang et al., 2012). Many researchers have conducted PFAS-induced hepatotoxicity using animal models (Fragki et al., 2021; Yen et al., 2024). However,

doi:10.6342/NTU202503955

conducting toxicological studies on each PFAS compound using animal models may be time-consuming, costly, and raise ethical concerns related to animal welfare.

In recent years, the scientific community has been dedicated to reducing the use of experimental animals due to ethical concerns. In 2016, the United States amended the Toxic Substances Control Act by adding a new subsection requiring the Environmental Protection Agency to develop alternative testing methods to reduce vertebrate animal testing (EPA, 2018). These strategies include the use of *in vitro* studies, which offer advantages such as lower cost, simpler sample preparation, and higher throughput compared to animal experiments.

Previous *in vitro* studies have linked PFAS to mitochondrial damage, increase oxidative stress, and alter the expression of genes involved in lipid metabolism (Li et al., 2025; Luo et al., 2024). These findings support the utility of *in vitro* systems, such as HepG2 cells, as effective platforms for elucidating PFAS-induced hepatotoxic mechanisms. Using *in vitro* may potentially provide substitute for *in vivo* models in early-stage toxicity screening, offering a faster and more efficient strategy for toxicological assessment.

1.7 Study aims

The aims of this study are to:

doi:10.6342/NTU202503955

(1) Understand the mechanism of PFOS induced cell toxicity by analyzing PC-CL changes in human hepatoma HepG2 cells exposed to a series dose of PFOS.

(2) Compare the changes of PC-CL profile caused by PFOS in of HepG2 cells with the results from animal models.

In this study, HepG2 cells were exposed to different concentrations of PFOS. The changes of PC-CL profile induced by PFOS were analyzed using ultra-performance liquid chromatography–triple quadrupole mass spectrometry (UPLC-MS/MS). The results of this study may provide insights into the mechanisms of PFOS-induced hepatotoxicity and potentially contribute to the development of a platform for PFAS toxicity assessment in the future.

doi:10.6342/NTU202503955

Chapter 2 Materials and methods

2.1 The study framework

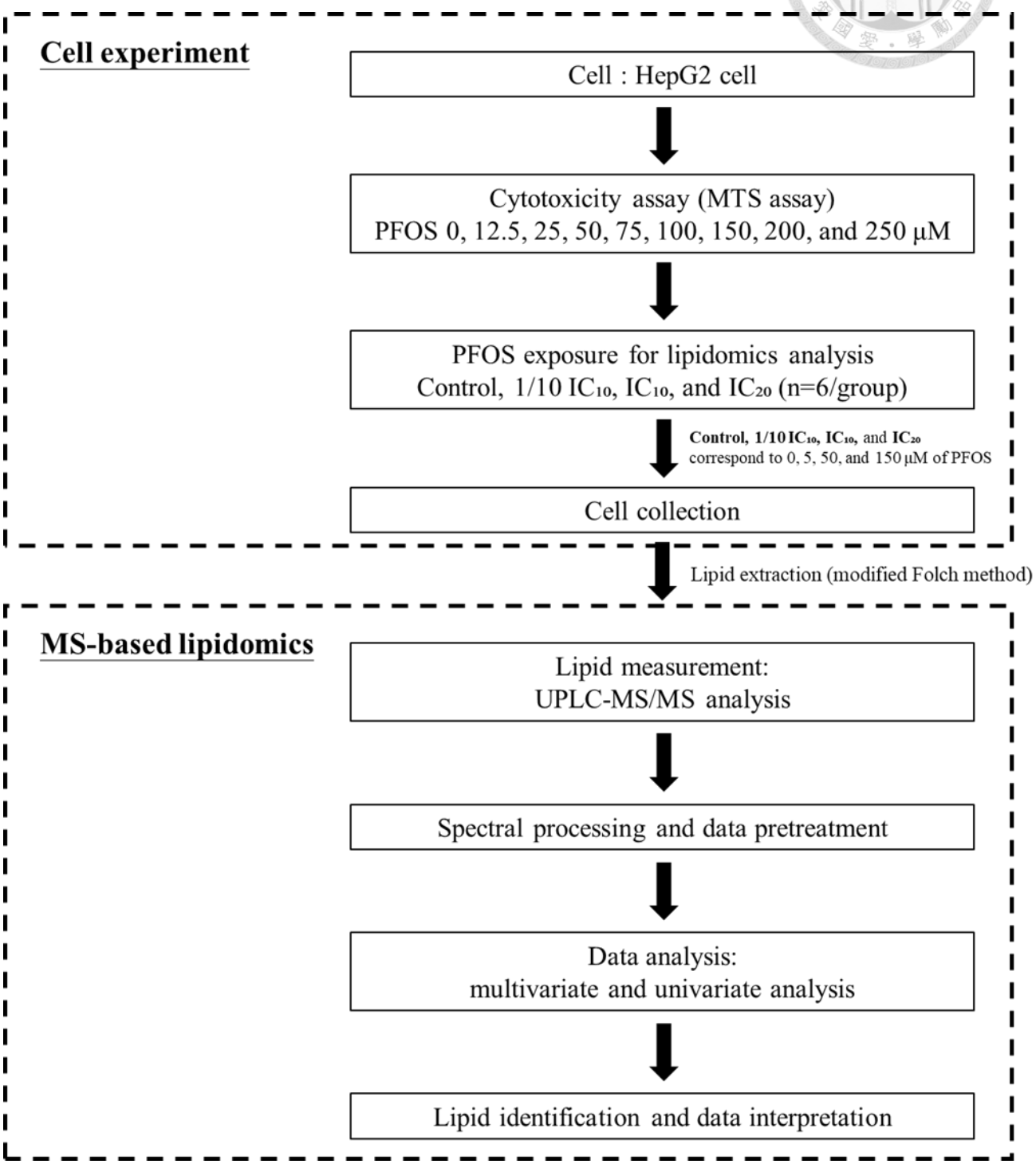

PFOS: Perfluorooctanesulfonic Acid

IC: Inhibitory concentration

UPLC-MS/MS: Ultra-performance liquid chromatography coupled with a triple quadrupole mass spectrometer

doi:10.6342/NTU202503955

2.2 HepG2 cells treated with PFOS

2.2.1 Chemicals

PFOS obtained from Sigma (St. Louis, MO, USA) was dissolved in dimethyl sulfoxide (DMSO). DMSO was also acquired from Sigma. Fetal bovine serum (FBS) was sourced from HyClone (Logan, UT, USA). Dulbecco's Modified Eagle's Medium (DMEM), penicillin, and streptomycin were purchased from Life Technologies (Gaithersburg, MD, USA). The MTS cell proliferation assay kit (ab197010) was obtained from Abcam (USA). All other reagents and solvents used were of analytical grade and bought from Sigma

2.2.2 HepG2 cells culture

Cell culture and maintenance and chemical treatment was based on previous literature (Chen et al., 2010; Chiang et al., 2011) and conducted in the laboratory of Prof. Su-yin Chiang at China Medical University, Taiwan. The human hepatoma cell line HepG2 was obtained from the Bioresource Collection and Research Center (Hsinchu, Taiwan). Cells were cultured in DMEM supplemented with 10% (v/v) heat-inactivated FBS, 100 U/mL penicillin, and 100 μg/mL streptomycin. Cultivation was performed in 75 cm^2 tissue culture flasks and maintained in a humidified incubator at 37°C with 5% CO_2 atmosphere, as previously described (Chiang et al., 2011).

doi:10.6342/NTU202503955

2.2.3 Cytotoxicity assessment

The PFOS concentration chosen for lipidomic analysis were determined based on the results of the cytotoxicity assessment (MTS cell viability assay). The MTS assay is a colorimetric method used to assess cell viability based on metabolic activity. It utilizes the tetrazolium compound MTS, which is reduced by NADH/NADPH-dependent dehydrogenase enzymes in viable cells to produce a soluble formazan product. This reduction process requires the presence of intermediate electron acceptors, typically phenazine methosulfate, to facilitate electron transfer. The resulting formazan can be directly quantified by measuring absorbance at 490–500 nm using a microplate reader. Since the reaction depends on mitochondrial and cytoplasmic enzymatic activity, the MTS assay provides a reliable indication of the metabolic status of living cells (Riss et al., 2016).

The HepG2 cells were seeded at a density of 0.5×10^4 cells per well in 96-well culture plates and incubated for 24 hours. The next day, cells were treated with 12.5, 25, 50, 75, 100, 150, 200, and 250 μM of PFOS or a DMSO vehicle control at final concentration not exceeding 0.1%).

After 48 hours of exposure, the cytotoxicity was determined using the MTS assay (Chiang et al., 2011).The cells were washed twice with 1× phosphate-buffered saline (PBS), followed by the addition of 20 μL MTS reagent to each well. Plates were then

doi:10.6342/NTU202503955

incubated at 37 °C in a CO_2 incubator for 3–4 hours, and absorbance was measured at 490 nm using a SpectraMax® 340PC384 microplate reader (Molecular Devices, Sunnyvale, CA, USA). The results are presented as the mean ± standard deviation (SD).

The cell viability was calculated using the following equation:

Cell viability (%) = [(Absorbance of PFOSs treated cells−Absorbance of medium only) / (Absorbance of DMSO-treated cells−Absorbance of medium only)] × 100%. The inhibitory concentration (IC) refers to the concentration of a chemical required to inhibit a specific biological activity or cellular function by a defined percentage. For instance, the IC_{10} value representing the concentration at which 10% inhibition of cell viability is observed. According to the ISO 10993-5:2009 and ISO 19007:2018 guidelines for *in vitro* cytotoxicity testing, a reduction in cell viability greater than 30% (i.e., cell viability below 70%) is considered indicative of a cytotoxic effect. Therefore, cell viability above 70% was deemed acceptable for subsequent biological evaluations to minimize interference from dead or damaged cells. In the current study, the concentrations corresponding to 1/10 of the IC_{10} (1/10 IC_{10}), IC_{10}, and IC_{20} were selected as the PFOS exposure levels for lipidomics analysis (Kovrlija et al., 2024).

doi:10.6342/NTU202503955

2.2.4 PFOS exposure for lipidomic analysis

HepG2 cells were seeded in 10-cm culture dishes and incubated overnight. On the following day, cells were treated with PFOS at concentrations corresponding to 1/10 IC_{10}, IC_{10}, and IC_{20} for 48 hours. Each concentration was tested in six replicates. Prior to cell collection, methanol and 1.5 mL microcentrifuge tubes were pre-cooled at −80°C for at least 1 hour. After 48 hours of PFOS exposure, the cells from control groups were observed under a microscope and were estimated to occupy about 70–80% of the culture surface, suggesting that the cells were in a favorable growth state suitable for downstream applications. Cells were then washed twice with 10 mL of 1× PBS. Subsequently, 10 mL of liquid nitrogen was added to each dish; after the nitrogen had fully evaporated, the dishes were transferred onto dry ice. Cells were then scraped using a cell scraper in 500 μL of pre-cooled methanol. The resulting cell suspension was transferred into 1.5 mL microcentrifuge tubes and stored at −80°C until further analysis.

2.3 LC-MS based lipidomic analysis

2.3.1 Sample preparation

A modified Folch extraction method was used to extract lipids from PFOS-treated HepG2 cells (Folch et al., 1957; Tang et al., 2011). Briefly, 400 μL of chloroform and 150 μL of 0.15 M NaCl were added to 200 μL of methanol containing HepG2 cells. The

doi:10.6342/NTU202503955

mixture was vortexed for 10 minutes and then centrifuged at 11,000 rpm for 10 minutes at 10 °C. The chloroform (bottom) layer was collected and evaporated to dryness using centrifugal evaporator. The resulting lipid residues were reconstituted in 200 μL of methanol containing internal standards including PC(13:0/13:0), PC(17:0/0:0), and SM(d18:1/17:0), at a concentration of 0.2 mg/L, for subsequent lipid profiling. To assess data quality, a pooled quality control (QC) sample was prepared by combining equal volumes of each sample and analyzed alongside the experimental samples within the same batch.

2.3.2 Lipid measurement through UPLC-MS/MS

PC-CL analysis were conducted using an ultra-performance liquid chromatography system coupled with a triple quadrupole mass spectrometer (UPLC-TQ-MS). Chromatographic separation was carried out on a BEH C18 column (100 mm × 2.1 mm i.d., 1.7 μm particle size; Waters, Milford, USA) using a binary solvent system: mobile phase A consisted of ultrapure water containing 10 mM ammonium acetate (NH_4Ac), while mobile phase B was a mixture of acetonitrile and methanol (65:35, v/v) also containing 10 mM NH_4Ac. The gradient elution began with 35% mobile phase B, which was ramped to 70% within 0.1 min, further increased to 100% by 1.4 min, maintained for 4.5 min, and then returned to 35% over 3 min. The flow rate

doi:10.6342/NTU202503955

and column temperature were held constant at 0.7 mL/min and 70°C, respectively. Mass spectrometric data were acquired using a precursor ion scan mode in positive ionization, targeting parent ions ($[M+H]^+$) that generate a characteristic fragment ion at m/z 184, specific to PC-CL (e.g., PCs and SMs). The ion source was operated under the following conditions: capillary voltage at 2.5 kV, desolvation gas (nitrogen) flow at 700 L/h and 450°C, and cone gas flow at 50 L/h with a source temperature of 120°C and cone voltage of 35 V. For collision-induced dissociation, argon was used as the collision gas at a flow rate of 0.1 mL/min with a collision energy of 30 eV. QC was ensured by periodically injecting pooled QC samples throughout each analytical batch.

2.3.3 Lipid identification

The detected signals corresponding to PCs and SMs were distinguished based on the nitrogen rule, while LPCs were initially separated from PCs by their characteristic retention times in the UPLC. Further structural identification of lipid species was conducted using an in-house lipid library based on retention time and mass-to-charge (m/z) ratio. For those PCs not in the in-house lipid library can be identified using product ion scan, including the $[M+H]^+$, $[M+Na]^+$, and $[M-Me]^-$ modes. The $[M+H]^+$ mode was operated under the same parameters as the precursor ion scan. The $[M+H]^+$ scan enabled subclass discrimination of LPC, whereas DPC subclasses were identified

doi:10.6342/NTU202503955

via sodium adducts in the $[M+Na]^+$ mode. Following subclass identification, the $[M-Me]^-$ mode was employed to determine the carbon number and degree of unsaturation of the fatty acid moieties.

2.3.4 Data preprocessing

The raw data obtained from UPLC–TQ-MS analysis were first converted into NetCDF format using MassLynx 4.1 (Waters, CA, USA). Data processing, including mass detection, chromatogram building, deconvolution, isotopic peak grouping, peak alignment, and gap filling, was performed using MZmine 4.0.3 to generate a data matrix containing detected peaks and their corresponding peak areas for each sample (Schmid et al., 2023).

The reproducibility of the analysis was evaluated through repeated measurements of QC samples at the beginning, middle, and end of the UPLC–TQ-MS analysis. The coefficient of variation (CV, %) was calculated for each detected peak, and peaks with CV values greater than 30% were excluded from further analysis to improve data quality (Want et al., 2013). This step helped reduce variability due to sample preparation, instrumental drift, and data processing errors. The remaining peak areas were normalized to the total peak area within each sample. Following spectral data

doi:10.6342/NTU202503955

processing, the unit variance scaling and log transformation was conducted to reduce systematic bias.

2.3.5 Statistical analysis

Multivariate statistical analyses including principal component analysis (PCA) and partial least squares discriminant analysis (PLS-DA) were performed to explore and characterize the lipid variations among treatment groups using SIMCA version 13.2 (Umetrics, Umeå, Sweden). PCA was applied to visualize overall data clustering and identify intrinsic patterns without supervision, while PLS-DA was used to enhance group separation and identify potential discriminative lipids. PCA was employed as an unsupervised analytical approach that does not require predefined treatment labels. It reduces the dimensionality of the dataset by generating principal components, which are linear combinations of the original variables, while preserving the maximum possible variance. The results were normally visualized in a two-dimensional score scatter plot, where the x- and y-axes represent the first two principal components (PC1 and PC2), respectively. This plot enables the identification of overall trends in lipid alterations, differentiation among sample clusters, and detection of outliers.

PLS-DA, in contrast, is a supervised method that incorporates prior class information to enhance group separation. It normally projects the data into a two-

doi:10.6342/NTU202503955

dimensional score plot to highlight inter-group differences. The quality of the PLS-DA model was assessed using the parameters R^2Y (goodness of fit) and Q^2 (predictive ability). A robust model was defined as one with $Q^2 > 0$, and $R^2Y - Q^2 < 0.3$, as previously described (Eriksson et al., 2013).

For univariate analysis, the Kruskal–Wallis test followed by Dunn's post hoc test was applied using R version 4.4.1 to identify lipids that significantly differed among treatment groups. A significance threshold of $p < 0.05$ was used. When the Kruskal–Wallis test yielded statistical significance, Dunn's test was subsequently performed to determine pairwise differences between groups. Additionally, fold-change analysis was conducted on significant lipids to assess the magnitude of changes between treatment and control groups within cell samples.

Chapter 3 Results

3.1 The MTS cytotoxicity assay for PFOS treatment

The effects on the cell viability in HepG2 cells after 48 h exposure to various concentrations of PFOS (0, 12.5, 25, 50, 75, 100, 150, 200, and 250 μM) were measured by MTS assay. The solvent controls (0.1% DMSO) do not affect the cell viability of the HepG2 cells. At 48 h exposure, the 1/10 IC_{10}, IC_{10} and IC_{20} values of PFOS in HepG2 cells were estimated to be about 50 μM, and 150 μM of PFOS, respectively **(Figure 5)**.

doi:10.6342/NTU202503955

The doses of 1/10 IC_{10}, IC_{10}, and IC_{20} of PFOS, corresponding to 5, 50, and 150 μM of PFOS, were chosen for metabolomic analysis.

3.2 PC-CL in HepG2 cells

The total ion chromatogram of the QC sample is presented in **(Figure 6)**. Among the 889 detected lipid features, 97 features met the criterion of having a CV below 30% across repeated measurements in the QC samples of PFOS-treated HepG2 cells. All 97 features were consistently observed in the control and PFOS treatment groups. These lipids were considered stable lipid features and were included for further analysis. The list of stable lipid features is presented in **(**錯誤! 找不到參照來源。**)**.

Among the 97 stably expressed lipid features **(**錯誤! 找不到參照來源。**)**, 85 features were identified as PCs and 12 as SMs. Of the 85 PCs, subclass identification revealed 2 LPCs, 49 DPCs, 3 O-PCs, and 8 P-PCs, while 23 PCs remained structurally unidentified. All 12 SMs were also unidentified at the structural level.

3.3 Multivariate analysis of PC-CL in response to PFOS treatments in HepG2 cells

The PCA score plot from the analysis of MS spectra of the HepG2 cells treated with PFOS is shown in **Figure 7**. Each data point corresponds to an individual sample.

doi:10.6342/NTU202503955

Due to an operation error, one sample from low-dose and one sample from medium-dose groups were lost, leaving only five samples in each group.

The repeated measurements of QC samples clustered tightly near the center of the PCA score plot, indicating stable performance of the UPLC-MS/MS system. Samples from the high-dose group were clearly separated from those of other treatment groups alone the second principal component, suggesting that high PFOS exposure may induce a distinct lipid response. Two samples from the medium-dose group were separated from the remaining three within the same group, possibly due to relatively low signal intensities, which may have introduced greater variance.

The PLS-DA score plot of MS analysis of HepG2 cells treated with PFOS is shown in **Figure 8**. The model shows moderate discrimination between groups, with the high-dose group clearly separated from the control and other dose groups along the LV1. The R^2Y value was 0.476 and the Q^2 value was 0.224. The $Q^2 > 0$ and $R^2Y - Q^2 < 0.3$ indicating a valid PLS-DA model.

3.4 Univariate analysis of PC-CL in response to PFOS treatments in HepG2 cells

The significantly altered lipids in PFOS-treated HepG2 cells, identified using the Kruskal–Wallis test are listed in **錯誤! 找不到參照來源。**. A total of 28 significantly

doi:10.6342/NTU202503955

altered lipids were identified, including 1 LPC, 18 DPCs, 3 ether-linked PCs (1 O-PC and 2 P-PCs), 4 unidentified PCs, and 2 unidentified SMs. Among these, PC(18:1/22:6), PC(20:4/20:4), and PC(20:5/22:5) showed a dose-dependent response, with lipid levels increasing as PFOS concentration increased.

The significantly altered lipids are shown in a heatmap **(Figure 9)**. The levels of DPCs changed in the high PFOS exposure group. Specifically, mono- and di-unsaturated DPCs were downregulated at high doses of PFOS, while polyunsaturated DPCs (PUFA-DPCs) were increased at medium and high doses. In addition, P-PC levels were increased in the high-dose group.

doi:10.6342/NTU202503955

Chapter 4 Discussion

4.1 Imbalance PC biosynthesis and lipid metabolism of HepG2 cells treated with various doses of PFOS

The altered PC species in HepG2 cells treated with various doses of PFOS were predominantly DPCs. Most mono- and di-unsaturated PCs were downregulated in the high-dose PFOS group, including PC(16:1/16:1), PC(16:0/17:1), and PC(16:0/18:2), whereas PUFA-PCs, such as PC(18:1/22:6) PC(20:4/20:4), and PC(20:5/22:5) were upregulated in the medium- and high-dose groups.

In the liver, PCs are primarily synthesized via two pathways: the CDP-choline pathway and the phosphatidylethanolamine N-methyltransferase (PEMT) pathway. The CDP-choline pathway is the dominant route, accounting for approximately 70–80% of hepatic PC biosynthesis. In this pathway, dietary choline is first phosphorylated to phosphocholine by choline kinase, then converted to CDP-choline by phosphocholine cytidylyltransferase. The final step is the transfer of choline from CDP-choline to diacylglycerol (DAG) catalyzed by 1,2-diacylglycerol choline phosphotransferase (CPT). In the PEMT pathway, the phosphatidylethanolamine (PE) is sequentially methylated to form PC through three methylation steps, catalyzed by PEMT (**Figure 10a)** (Li & Vance, 2008; van der Veen et al., 2017).

doi:10.6342/NTU202503955

The liver DPCs species synthesized from CDP-choline pathway were mainly mono- or di- unsaturated PCs, whereas the liver DPCs species synthesized from PEMT pathway were mainly PUFA-DPCs, especially the docosahexaenoic acid (DHA; 22:6n3). (DeLong et al., 1999). The observed downregulation of mono- and di-unsaturated DPCs, accompanied by the upregulation of PUFA-DPCs in PFOS-treated HepG2 cells, suggests that PFOS exposure may affect both the CDP-choline and PEMT pathways.

Previous studies found that PFOS can form an ion pair with two choline molecules in phosphate-buffered saline (Zhang et al., 2016). The formation of PFOS-choline ion pair reduces the bioavailable choline (Bagley et al., 2017), therefore reduce the formation of PCs species from CDP-choline pathway. The upregulation of the PEMT pathway may serve as a compensatory mechanism for the suppressed CDP-choline pathway to maintain PCs homeostasis (Yen et al., 2024). Cui and Vance (1996) found that mice fed with choline deficient diet for three weeks showed 2-fold increase of PEMT activity, suggested that PEMT pathway activity is associated with the level of bioavailable choline **(Figure 10b)**.

The imbalance PC biosynthesis may affect the VLDL secretion. During VLDL assembly in the liver, apoB serves as the structural backbone for the nascent lipoprotein particle. As apoB is synthesized and translocated into the ER, it initiates the recruitment

doi:10.6342/NTU202503955

of lipids, particularly TG and phospholipids. PCs stabilize the lipid monolayer of the VLDL particle and ensuring proper lipidation of apoB. Adequate levels of PC from both CDP-choline pathway and PEMT pathway are essential for the efficient assembly and secretion of VLDL. In conditions of PC deficiency, incomplete lipidation of apoB leads to its misfolding and subsequent degradation, impairing VLDL secretion. Therefore, PC availability directly influences the fate of apoB and the hepatic export of lipids via VLDL (Yao & Vance, 1988). The reduced VLDL secretion causes decreased lipid transportation from liver to peripheral tissue, leading to lipid accumulation in liver, which is the phenotype of NAFLD.

These findings suggest that alterations of PUFA-DPCs levels in high dose group of PFOS treated HepG2 cells in our study may indicate a compensatory mechanism of down-regulated mono-, and di-unsaturated DPCs. Moreover, the perturbed DPCs level may serve as a potential biomarker for hepatic lipid accumulation.

4.2 PFOS-induced hepatotoxicity through inflammatory response

PCs play roles in anti-inflammatory, antioxidant, and anti-fibrotic effects (Akin et al., 2007). In our study, several essential fatty acid (EFA)-containing DPCs including species incorporating arachidonic acid (AA; 20:4n-6), eicosapentaenoic acid (EPA;

doi:10.6342/NTU202503955

20:5n-3), and docosahexaenoic acid (DHA; 22:6n-3), were elevated in PFOS-treated HepG2 cells. All of those lipids are known to modulate inflammatory responses.

Previous studies showed that PFAS exposure may be associated metabolic pathways indicating oxidative stress and inflammatory responses, including the prostaglandin formation from AA metabolism (Alijagic et al., 2024). Moreover, PFAS was found to be associated with protein level of NF-κB, indicating an immune effect (Khan et al., 2023).

AA and EPA are commonly incorporated into membrane phospholipids such as PCs. Upon exposure to inflammatory stimuli, phospholipase A2 is activated and cleaves these fatty acids from the membrane, releasing free AA or EPA (Dennis, 2016). These free PUFAs serve as key substrates for multiple enzymatic pathways involved in inflammation, particularly the cyclooxygenase (COX) and lipoxygenase (LOX) pathways, leading to the production of various bioactive lipid mediators.

The COX pathway converts AA into 2-series prostanoids, which exert pro-inflammatory effects. In contrast, EPA-derived 3-series prostanoids may competitively inhibit AA metabolism by COX, thereby exerting anti-inflammatory effects (Norris & Dennis, 2012). In the LOX pathway, AA and EPA are converted into 4-series (AA-derived) and 5-series (EPA-derived) leukotrienes, respectively, as well as lipoxins (Sala et al., 2018). DHA can be converted into maresin 1-2, protectin D1, and resolvins D1–

doi:10.6342/NTU202503955

D6 through the LOX pathway **(Figure 11)**. LOX-derived mediators from AA generally exert pro-inflammatory responses, whereas mediators derived from EPA and DHA exert anti-inflammatory effects either by competitively binding to LOX enzymes, thus inhibiting AA metabolism, or by directly suppressing the NF-κB signaling pathway (Lee et al., 2003; Serhan, 2014).

In summary, the elevated levels of EFA-containing DPCs observed in PFOS-treated HepG2 cells may reflect a complex inflammatory response possibly involving both the biosynthesis of lipid mediators through both COX and LOX pathways, as well as the concurrent activation of pro-resolving and anti-inflammatory signaling pathway.

4.3 PFOS-induced hepatotoxicity through oxidative stress and membrane damage

In our study, the up-regulated ether-linked PCs, such as PC(P-16:1/20:3) and PC(P-20:5/18:0), were observed in HepG2 cells treated with a high dose of PFOS. The increase in P-PCs may indicate a protective cellular response against PFOS-induced oxidative stress and membrane damage. P-PCs are known to function as endogenous antioxidants due to their vinyl ether bond, which is particularly susceptible to oxidation by ROS, thereby protecting other membrane lipids from oxidative degradation.

doi:10.6342/NTU202503955

Additionally, ether-linked PCs are involved in stabilizing membrane structure, enhancing bilayer rigidity, and preserving membrane integrity under stress conditions.

Previous studies have reported altered P-PC levels in the liver lipidome of male ICR mice treated with naphthalene and male SD rats exposed to $PM_{2.5}$ .The altered P-PC level indicated oxidative stress caused by toxicant (Lin et al., 2021; Ling et al., 2014). It has also been found that P-PC supplementation may alleviate oxidative stress in the liver. A previous study demonstrated that P-PC supplementation prevented the development of steatosis in mice fed a high-fat diet by activating PPAR signaling pathway (Jang et al., 2017). Similarly, Mei et al. (2024) reported that AML12 hepatocytes supplemented with P-PC showed reduced oxidative stress induced by CCl_4. Elevated levels of glutathione and increased activity of glutathione peroxidase were observed, along with decreased MDA levels, indicating enhanced antioxidant capacity and reduced oxidative stress in the P-PC supplementation group. Moreover, CCl_4-treated AML12 hepatocytes with P-PC supplementation maintained more intact plasma membranes compared to those without supplementation, suggesting a membrane-protective effect of P-PC.

The elevation of P-PCs in HepG2 cells treated with a high dose of PFOS may reflect an adaptive response to reduce oxidative stress and maintain cellular homeostasis. As PFOS is known to induce ROS production and promote membrane

doi:10.6342/NTU202503955

lipid peroxidation (Kashobwe et al., 2024), the upregulation of P-PCs may serve to mitigate oxidative damage and help preserve membrane stability under PFOS-induced oxidative stress.

4.4 Comparison of the results with previous PFOS *in vitro* studies

Several *in vitro* studies have been conducted to investigate the hepatotoxic mechanisms of PFOS exposure using various liver-derived cell models. We compare the effects of PFOS on PC-CL profile in HepG2 cells with the results from other *in vitro* studies to elucidate whether specific lipid alterations may explain previously observed biochemical outcomes.

The disrupted CDP-choline and PEMT pathway in our study may partly explain the mechanism of significantly increased TG concentration in HepaRG cell treated with 6.25, 12.5, 25, 50, 100, 200, and 400 μM of PFOS for 24 hours in previous study (Louisse et al., 2020). VLDL is responsible for transporting lipids from the liver to peripheral tissues. Changes in DPC species derived from both the CDP-choline and PEMT pathways may impair VLDL assembly and secretion (Vance, 2014), which may cause the decreased TG transportation by VLDL, leading to TG accumulation.

Li et al. (2025) examined PFOS toxicity effect on lipid metabolism by treating HepG2 cells with 50, 100, 200, and 400 μM of PFOS for 24 hours and measured the

doi:10.6342/NTU202503955

lipidome along with the oxidative stress biomarker. The result of pathway analysis indicated that the highest concentration (400 μM) of PFOS induced down-regulation in choline metabolism. The downregulation of mono- and di-unsaturated DPCs observed in our study may reflect a similar effect, as increased PEMT activity has previously been reported under conditions of choline deficiency. A significant increase in ROS levels at PFOS concentrations of 200 μM and above was observed in that study. Notably, 200 μM PFOS corresponds to the IC_{30} in our MTS assay. It has been reported that ROS leads to cell death (Matic, 2018). The significantly increased ROS level at 200 μM PFOS and above in Li et al. (2025)'s study, which is equal to IC_{30} and above in our study, may be attributed to the depletion of EFA-containing DPCs at PFOS concentrations higher than those used in our study. At very high doses of PFOS exposure, the hepatoprotective capacity of HepG2 cells may become insufficient to counteract ROS accumulation, resulting in sharply elevated ROS levels and a marked decline in cell viability due to oxidative stress.

These *in vitro* studies suggest that PFOS exposure, even at concentrations below the cytotoxicity threshold, may induce hepatic lipid accumulation, likely through impaired VLDL secretion or altered phospholipid metabolism. At moderately high concentrations, PFOS may also trigger compensatory hepatoprotective responses, such as the increased level of antioxidant lipid species. However, at very high concentrations

doi:10.6342/NTU202503955

(≥200 μM on HepG2 cells), the antioxidant defense may not be able to clear the excessive ROS accumulation, leading to a marked decrease in cell viability due to oxidative stress. Moreover, despite variations in exposure duration and metabolic activity between HepG2 and HepaRG cells, the observed lipid alterations, including DPC remodeling and TG accumulation, were consistent across studies. This suggests that such factors may not critically influence the fundamental mechanisms of PFOS-induced lipid dysregulation.

4.5 Comparison of the lipid results with previous PFOS studies using animal models

The pattern of lipid alteration by PFOS in HepG2 cells in this study was similar to the results in the liver of BALB/c mice treated with PFOS for 2 months (Li et al., 2021), characterized by increased PUFA-DPCs level in the 1000 μg/kg/day group, which was the highest PFOS exposure concentration in their study. However, the lipid changes observed in this *in vitro* study were distinct from those in our previous animal studies (Yen et al., 2024). In our previous study, male SD rats were treated with 0, 5, and 10 mg/kg/day of PFOS administered via gavage for 21days. Some PUFA-DPCs, such as the 20:5 (EPA)-containing PCs, were upregulated in the 10 mg/kg/day group, consistent with the findings of our current study. However, the decreased 22:6 (DHA)-containing

doi:10.6342/NTU202503955

PCs and P-PCs in the liver of 10 mg/kg/day PFOS exposure group were opposite to the current study.

DHA may exert anti-inflammatory effect, whereas P-PCs may play roles in anti-oxidation. At lower PFOS concentration, the increased PUFA-DPCs may imply an adaptive compensatory response aimed at mitigating inflammatory response, preserving membrane fluidity, and counteracting oxidative stress. However, under higher PFOS exposure, excessive ROS generation and lipid peroxidation may drive the depletion of P-PC or highly unsaturated phospholipids such as DHA-containing DPCs. This toxic mechanism aligns with findings from NAFLD models, where lipotoxicity-induced ROS overproduction accelerates PUFA peroxidation and depletes DHA levels, contributing to hepatic injury and disease progression (Svegliati-Baroni et al., 2019).

These findings suggest that at relatively low doses of PFOS exposure, HepG2 cells showed both anti-inflammatory and antioxidative responses. In contrast, under higher PFOS exposure conditions, as shown in our previous animal study, depletion of EPA- and DHA-containing DPCs, as well as P-PCs, was observed—likely due to elevated immune activation and oxidative stress that exceeded the cellular recovery capacity.

4.6 The contribution and the limitation

doi:10.6342/NTU202503955

This study provides insights into the lipid alterations induced by PFOS in HepG2 cells and highlights the potential of *in vitro* models as alternatives to animal testing, particularly under conditions of relatively low PFOS exposure. In this study, sublethal doses of PFOS caused changes in lipid profiles, such as the elevation of PUFA-containing DPCs and ether-linked PCs, which are indicative of early-stage cellular responses to moderate oxidative stress. These findings support the application of lipidomics to *in vitro* toxicity studies for suggesting possible hepatotoxic mechanisms, enabling a more ethical, cost-effective, and high-throughput platform compared to *in vivo* studies.

However, there are limitations to this model. Among the 889 detected lipid features, only few features met the criterion of having a CV below 30% across repeated measurements in the QC samples, possible due to the low original abundance of some lipids after MS measurement, which leads to greater variability. Given that PC-CL represents only a subset of the entire lipid profile, potential changes in other lipid classes may have been overlooked. Future studies employing untargeted lipidomic approaches may enable a more comprehensive assessment of PFOS-induced lipid perturbations across diverse lipid species and metabolic pathways. Moreover, HepG2 cells, which are derived from hepatocellular carcinoma, have limited liver-specific functions and lower metabolic activity compared to primary human hepatocytes or

doi:10.6342/NTU202503955

HepaRG cells, particularly in terms of enzyme expression such as cytochrome P450 activity (Bonanini et al., 2024). This may limit their ability to fully replicate xenobiotic metabolism and long-term hepatotoxic outcomes. Lastly, the exposure concentrations used in this study were relatively low, which may limit the extrapolation of results to more severe exposure scenarios in animal models. Therefore, while our study contributes to the replacement and reduction of animal testing, further interpretation of high-concentration PFOS exposure should be approached with caution.

Chapter 5 Conclusion

In this study, a MS-based lipidomic approach was employed to investigate the effects of PFOS exposure on PC-CLs in HepG2 cells. Based on cytotoxicity testing, three exposure concentrations, 1/10 IC_{10}, IC_{10} and $IC_{20,}$ were selected for further lipidomic analysis. Using UPLC–TQ-MS and statistical analysis, 28 significantly altered lipids were identified, with DPCs being the most affected class. Among these, several PUFA-DPCs, including PC(18:1/22:6), PC(20:4/20:4), and PC(20:5/22:5), showed a dose-dependent increase, while mono- and di-unsaturated DPCs were decreased under high-dose PFOS exposure. In addition, P-PCs were also elevated in the high-dose group.

doi:10.6342/NTU202503955

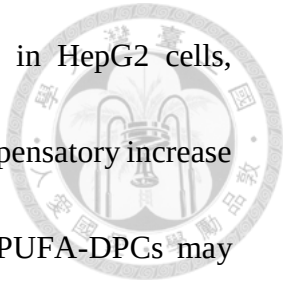

These findings suggest that PFOS disrupts PC biosynthesis in HepG2 cells, potentially impairing the CDP-choline pathway and leading to a compensatory increase in PUFA-DPCs via the PEMT pathway. Moreover, the elevated PUFA-DPCs may reflect an enhanced inflammatory response, as these lipids are key precursors for pro- and anti-inflammatory mediators generated through the COX and LOX pathways. The accumulation of P-PCs under high PFOS exposure further indicates a possible adaptive mechanism to counteract oxidative stress and maintain membrane integrity.

These findings suggest that lipidomic analysis of PC-CL using HepG2 cells may have potential to serve as a partial alternative to *in vivo* models, for assessing the effects of low-dose PFOS exposure.

doi:10.6342/NTU202503955

References

Akin, M., Demirbilek, S., Ay, S., Gurunluoglu, K., Turkmen, E., Tas, E., Aksoy, R. T., Baykarabulut, A., & Edali, M. N. (2007). Attenuation of ureteral obstruction-induced renal injury by polyenylphosphatidylcholine. *Int J Urol*, *14*(4), 350-356. https://doi.org/10.1111/j.1442-2042.2006.01717.x

Alderete, T. L., Jin, R., Walker, D. I., Valvi, D., Chen, Z., Jones, D. P., Peng, C., Gilliland, F. D., Berhane, K., Conti, D. V., Goran, M. I., & Chatzi, L. (2019). Perfluoroalkyl substances, metabolomic profiling, and alterations in glucose homeostasis among overweight and obese Hispanic children: A proof-of-concept analysis. *Environ Int*, *126*, 445-453. https://doi.org/10.1016/j.envint.2019.02.047

Alijagic, A., Sinisalu, L., Duberg, D., Kotlyar, O., Scherbak, N., Engwall, M., Oresic, M., & Hyotylainen, T. (2024). Metabolic and phenotypic changes induced by PFAS exposure in two human hepatocyte cell models. *Environ Int*, *190*, 108820. https://doi.org/10.1016/j.envint.2024.108820

Amstutz, V. H., Cengo, A., Gehres, F., Sijm, D., & Vrolijk, M. F. (2022). Investigating the cytotoxicity of per- and polyfluoroalkyl substances in HepG2 cells: A structure-activity relationship approach. *Toxicology*, *480*, 153312. https://doi.org/10.1016/j.tox.2022.153312

Bagley, B. D., Chang, S.-C., Ehresman, D. J., Eveland, A., Zitzow, J. D., Parker, G. A., Peters, J. M., Wallace, K. B., & Butenhoff, J. L. (2017). Perfluorooctane sulfonate-induced hepatic steatosis in male Sprague Dawley rats is not attenuated by dietary choline supplementation. *Toxicological sciences*, *160*(2), 284-298.

Bonanini, F., Singh, M., Yang, H., Kurek, D., Harms, A. C., Mardinoglu, A., & Hankemeier, T. (2024). A comparison between different human hepatocyte models reveals profound differences in net glucose production, lipid composition and metabolism in vitro. *Exp Cell Res*, *437*(1), 114008. https://doi.org/10.1016/j.yexcr.2024.114008

Brusseau, M. L., Anderson, R. H., & Guo, B. (2020). PFAS concentrations in soils: Background levels versus contaminated sites. *Sci Total Environ*, *740*, 140017. https://doi.org/10.1016/j.scitotenv.2020.140017

Butenhoff, J. L., Chang, S.-C., Olsen, G. W., & Thomford, P. J. (2012). Chronic dietary toxicity and carcinogenicity study with potassium perfluorooctanesulfonate in Sprague Dawley rats. *Toxicology*, *293*(1-3), 1-15.

Chang, S.-C., Noker, P. E., Gorman, G. S., Gibson, S. J., Hart, J. A., Ehresman, D. J., & Butenhoff, J. L. (2012). Comparative pharmacokinetics of perfluorooctanesulfonate (PFOS) in rats, mice, and monkeys. *Reproductive Toxicology*, *33*(4), 428-440.

Chen, Y. Y., Chung, J. G., Wu, H. C., Bau, D. T., Wu, K. Y., Kao, S. T., Hsiang, C. Y., Ho, T. Y., & Chiang, S. Y. (2010). Aristolochic acid suppresses DNA repair and triggers oxidative DNA damage in human kidney proximal tubular cells. *Oncol Rep*, *24*(1), 141-153. https://doi.org/10.3892/or_00000839

Chiang, S. Y., Lee, P. Y., Lai, M. T., Shen, L. C., Chung, W. S., Huang, H. F., Wu, K. Y., & Wu, H. C. (2011). Safrole-2',3'-oxide induces cytotoxic and genotoxic effects in HepG2 cells and in mice. *Mutat Res*, *726*(2), 234-241. https://doi.org/10.1016/j.mrgentox.2011.09.014

Control, C. f. D., & Prevention. (2022). Biomonitoring data tables for environmental chemicals. In.

Cui, Z., & Vance, D. E. (1996). Expression of phosphatidylethanolamine N-methyltransferase-2 is markedly enhanced in long term choline-deficient rats. *J Biol Chem*, *271*(5), 2839-2843. https://doi.org/10.1074/jbc.271.5.2839

Darrow, L. A., Groth, A. C., Winquist, A., Shin, H.-M., Bartell, S. M., & Steenland, K. (2016). Modeled perfluorooctanoic acid (PFOA) exposure and liver function

doi:10.6342/NTU202503955

in a Mid-Ohio Valley community. *Environmental health perspectives*, *124*(8), 1227-1233.
Dehghani, M. H., Aghaei, M., Bashardoust, P., Rezvani Ghalhari, M., Nayeri, D., Malekpoor, M., Sheikhi, S., & Shi, Z. (2025). An insight into the environmental and human health impacts of per- and polyfluoroalkyl substances (PFAS): exploring exposure pathways and their implications. *Environmental Sciences Europe*, *37*(1). https://doi.org/10.1186/s12302-025-01122-9
DeLong, C. J., Shen, Y. J., Thomas, M. J., & Cui, Z. (1999). Molecular distinction of phosphatidylcholine synthesis between the CDP-choline pathway and phosphatidylethanolamine methylation pathway. *J Biol Chem*, *274*(42), 29683-29688. https://doi.org/10.1074/jbc.274.42.29683
Dennis, E. A. (2016). Liberating Chiral Lipid Mediators, Inflammatory Enzymes, and LIPID MAPS from Biological Grease. *J Biol Chem*, *291*(47), 24431-24448. https://doi.org/10.1074/jbc.X116.723791
EPA, U. (2018). Strategic plan to promote the development and implementation of alternative test methods within the TSCA program. *US Environmental Protection Agency, Office of Chemical Safety and Pollution Prevention*.
Eriksen, K. T., Raaschou-Nielsen, O., McLaughlin, J. K., Lipworth, L., Tjonneland, A., Overvad, K., & Sorensen, M. (2013). Association between plasma PFOA and PFOS levels and total cholesterol in a middle-aged Danish population. *PLoS One*, *8*(2), e56969. https://doi.org/10.1371/journal.pone.0056969
Eriksson, L., Byrne, T., Johansson, E., Trygg, J., & Vikström, C. (2013). *Multi-and megavariate data analysis basic principles and applications* (Vol. 1). Umetrics Academy.
Evich, M. G., Davis, M. J. B., McCord, J. P., Acrey, B., Awkerman, J. A., Knappe, D. R. U., Lindstrom, A. B., Speth, T. F., Tebes-Stevens, C., Strynar, M. J., Wang, Z., Weber, E. J., Henderson, W. M., & Washington, J. W. (2022). Per- and polyfluoroalkyl substances in the environment. *Science*, *375*(6580), eabg9065. https://doi.org/10.1126/science.abg9065
Fahy, E., Cotter, D., Sud, M., & Subramaniam, S. (2011). Lipid classification, structures and tools. *Biochim Biophys Acta*, *1811*(11), 637-647. https://doi.org/10.1016/j.bbalip.2011.06.009
Fahy, E., Subramaniam, S., Brown, H. A., Glass, C. K., Merrill, A. H., Jr., Murphy, R. C., Raetz, C. R., Russell, D. W., Seyama, Y., Shaw, W., Shimizu, T., Spener, F., van Meer, G., VanNieuwenhze, M. S., White, S. H., Witztum, J. L., & Dennis, E. A. (2005). A comprehensive classification system for lipids. *J Lipid Res*, *46*(5), 839-861. https://doi.org/10.1194/jlr.E400004-JLR200
Fasano, W., Kennedy, G., Szostek, B., Farrar, D., Ward, R., Haroun, L., & Hinderliter, P. (2005). Penetration of ammonium perfluorooctanoate through rat and human skin in vitro. *Drug and Chemical Toxicology*, *28*(1), 79-90.
Fenton, S. E., Ducatman, A., Boobis, A., DeWitt, J. C., Lau, C., Ng, C., Smith, J. S., & Roberts, S. M. (2021). Per- and Polyfluoroalkyl Substance Toxicity and Human Health Review: Current State of Knowledge and Strategies for Informing Future Research. *Environ Toxicol Chem*, *40*(3), 606-630. https://doi.org/10.1002/etc.4890
Fiehn, O. (2001). Combining genomics, metabolome analysis, and biochemical modelling to understand metabolic networks. *Comparative and functional genomics*, *2*(3), 155-168.
Folch, J., Lees, M., & Stanley, G. H. S. (1957). A Simple Method for the Isolation and Purification of Total Lipides from Animal Tissues. *Journal of Biological Chemistry*, *226*(1), 497-509. https://doi.org/10.1016/s0021-9258(18)64849-5
Fragki, S., Dirven, H., Fletcher, T., Grasl-Kraupp, B., Bjerve Gutzkow, K., Hoogenboom, R., Kersten, S., Lindeman, B., Louisse, J., Peijnenburg, A., Piersma, A. H., Princen, H. M. G., Uhl, M., Westerhout, J., Zeilmaker, M. J., & Luijten, M. (2021). Systemic PFOS and PFOA exposure and disturbed lipid homeostasis in humans: what do we know and what not? *Crit Rev Toxicol*, *51*(2), 141-164. https://doi.org/10.1080/10408444.2021.1888073

doi:10.6342/NTU202503955

Gaines, L. G. T., Sinclair, G., & Williams, A. J. (2023). A proposed approach to defining per- and polyfluoroalkyl substances (PFAS) based on molecular structure and formula. *Integr Environ Assess Manag*, *19*(5), 1333-1347. https://doi.org/10.1002/ieam.4735

Gao, Y., Fu, J., Cao, H., Wang, Y., Zhang, A., Liang, Y., Wang, T., Zhao, C., & Jiang, G. (2015). Differential accumulation and elimination behavior of perfluoroalkyl Acid isomers in occupational workers in a manufactory in China. *Environ Sci Technol*, *49*(11), 6953-6962. https://doi.org/10.1021/acs.est.5b00778

Gathungu, R. M., Kautz, R., Kristal, B. S., Bird, S. S., & Vouros, P. (2020). The integration of LC-MS and NMR for the analysis of low molecular weight trace analytes in complex matrices. *Mass Spectrom Rev*, *39*(1-2), 35-54. https://doi.org/10.1002/mas.21575

Gluge, J., Scheringer, M., Cousins, I. T., DeWitt, J. C., Goldenman, G., Herzke, D., Lohmann, R., Ng, C. A., Trier, X., & Wang, Z. (2020). An overview of the uses of per- and polyfluoroalkyl substances (PFAS). *Environ Sci Process Impacts*, *22*(12), 2345-2373. https://doi.org/10.1039/d0em00291g

Goodrum, P. E., Anderson, J. K., Luz, A. L., & Ansell, G. K. (2021). Application of a framework for grouping and mixtures toxicity assessment of PFAS: A closer examination of dose-additivity approaches. *Toxicological sciences*, *179*(2), 262-278.

Guo, J., Wu, P., Cao, J., Luo, Y., Chen, J., Wang, G., Guo, W., Wang, T., & He, X. (2019). The PFOS disturbed immunomodulatory functions via nuclear Factor-kappaB signaling in liver of zebrafish (Danio rerio). *Fish Shellfish Immunol*, *91*, 87-98. https://doi.org/10.1016/j.fsi.2019.05.018

Jain, R. B. (2019). Concentration of selected liver enzymes across the stages of glomerular function: the associations with PFOA and PFOS. *Heliyon*, *5*(7), e02168. https://doi.org/10.1016/j.heliyon.2019.e02168

Jane, L. E. L., Yamada, M., Ford, J., Owens, G., Prow, T., & Juhasz, A. (2022). Health-related toxicity of emerging per- and polyfluoroalkyl substances: Comparison to legacy PFOS and PFOA. *Environ Res*, *212*(Pt C), 113431. https://doi.org/10.1016/j.envres.2022.113431

Jang, J. E., Park, H. S., Yoo, H. J., Baek, I. J., Yoon, J. E., Ko, M. S., Kim, A. R., Kim, H. S., Park, H. S., Lee, S. E., Kim, S. W., Kim, S. J., Leem, J., Kang, Y. M., Jung, M. K., Pack, C. G., Kim, C. J., Sung, C. O., Lee, I. K.,…Lee, K. U. (2017). Protective role of endogenous plasmalogens against hepatic steatosis and steatohepatitis in mice. *Hepatology*, *66*(2), 416-431. https://doi.org/10.1002/hep.29039

Jian, J. M., Chen, D., Han, F. J., Guo, Y., Zeng, L., Lu, X., & Wang, F. (2018). A short review on human exposure to and tissue distribution of per- and polyfluoroalkyl substances (PFASs). *Sci Total Environ*, *636*, 1058-1069. https://doi.org/10.1016/j.scitotenv.2018.04.380

Kannan, K., Corsolini, S., Falandysz, J., Fillmann, G., Kumar, K. S., Loganathan, B. G., Mohd, M. A., Olivero, J., Wouwe, N. V., & Yang, J. H. (2004). Perfluorooctanesulfonate and related fluorochemicals in human blood from several countries. *Environmental Science & Technology*, *38*(17), 4489-4495.

Kashobwe, L., Sadrabadi, F., Brunken, L., Coelho, A., Sandanger, T. M., Braeuning, A., Buhrke, T., Oberg, M., Hamers, T., & Leonards, P. E. G. (2024). Legacy and alternative per- and polyfluoroalkyl substances (PFAS) alter the lipid profile of HepaRG cells. *Toxicology*, *506*, 153862. https://doi.org/10.1016/j.tox.2024.153862

Kersten, S., & Stienstra, R. (2017). The role and regulation of the peroxisome proliferator activated receptor alpha in human liver. *Biochimie*, *136*, 75-84. https://doi.org/10.1016/j.biochi.2016.12.019

Khan, E. A., Gronnestad, R., Krokje, A., Bartosov, Z., Johanson, S. M., Muller, M. H. B., & Arukwe, A. (2023). Alteration of hepato-lipidomic homeostasis in A/J mice fed an environmentally relevant PFAS mixture. *Environ Int*, *173*, 107838. https://doi.org/10.1016/j.envint.2023.107838

doi:10.6342/NTU202503955

Khanna, R. K., Catanese, S., Emond, P., Corcia, P., Blasco, H., & Pisella, P.-J. (2022). Metabolomics and lipidomics approaches in human tears: A systematic review. *Survey of ophthalmology*, *67*(4), 1229-1243.
Kovrlija, I., Menshikh, K., Abreu, H., Cochis, A., Rimondini, L., Marsan, O., Rey, C., Combes, C., Locs, J., & Loca, D. (2024). Challenging applicability of ISO 10993-5 for calcium phosphate biomaterials evaluation: Towards more accurate in vitro cytotoxicity assessment. *Biomaterials Advances*, *160*, 213866.
Lee, J. Y., Ye, J., Gao, Z., Youn, H. S., Lee, W. H., Zhao, L., Sizemore, N., & Hwang, D. H. (2003). Reciprocal Modulation of Toll-like Receptor-4 Signaling Pathways Involving MyD88 and Phosphatidylinositol 3-Kinase/AKT by Saturated and Polyunsaturated Fatty Acids. *Journal of Biological Chemistry*, *278*(39), 37041-37051. https://doi.org/10.1074/jbc.M305213200
Li, X., Jing, K., He, L., Song, P., & Yu, J. (2025). Impact of per- and polyfluoroalkyl substances structure on oxidative stress and lipid metabolism disruption in HepG2 cells. *Toxicology*, *517*, 154218. https://doi.org/10.1016/j.tox.2025.154218
Li, X., Li, T., Wang, Z., Wei, J., Liu, J., Zhang, Y., & Zhao, Z. (2021). Distribution of perfluorooctane sulfonate in mice and its effect on liver lipidomic. *Talanta*, *226*, 122150. https://doi.org/10.1016/j.talanta.2021.122150
Li, Z., & Vance, D. E. (2008). Phosphatidylcholine and choline homeostasis. *J Lipid Res*, *49*(6), 1187-1194. https://doi.org/10.1194/jlr.R700019-JLR200
Lin, C. Y., Chen, W. L., Chen, T. Z., Lee, S. H., Liang, H. J., Chou, C. C., Tang, C. H., & Cheng, T. J. (2021). Lipid changes in extrapulmonary organs and serum of rats after chronic exposure to ambient fine particulate matter. *Sci Total Environ*, *784*, 147018. https://doi.org/10.1016/j.scitotenv.2021.147018
Ling, Y. S., Liang, H. J., Chung, M. H., Lin, M. H., & Lin, C. Y. (2014). NMR- and MS-based metabolomics: various organ responses following naphthalene intervention. *Mol Biosyst*, *10*(7), 1918-1931. https://doi.org/10.1039/c4mb00090k
Louisse, J., Rijkers, D., Stoopen, G., Janssen, A., Staats, M., Hoogenboom, R., Kersten, S., & Peijnenburg, A. (2020). Perfluorooctanoic acid (PFOA), perfluorooctane sulfonic acid (PFOS), and perfluorononanoic acid (PFNA) increase triglyceride levels and decrease cholesterogenic gene expression in human HepaRG liver cells. *Arch Toxicol*, *94*(9), 3137-3155. https://doi.org/10.1007/s00204-020-02808-0
Luo, Y. S., Ying, R. Y., Chen, X. T., Yeh, Y. J., Wei, C. C., & Chan, C. C. (2024). Integrating high-throughput phenotypic profiling and transcriptomic analyses to predict the hepatosteatosis effects induced by per- and polyfluoroalkyl substances. *J Hazard Mater*, *469*, 133891. https://doi.org/10.1016/j.jhazmat.2024.133891
Malhotra, P., Gill, R. K., Saksena, S., & Alrefai, W. A. (2020). Disturbances in cholesterol homeostasis and non-alcoholic fatty liver diseases. *Frontiers in Medicine*, *7*, 467.
Martínez-Uña, M., Varela-Rey, M., Cano, A., Fernández-Ares, L., Beraza, N., Aurrekoetxea, I., Martínez-Arranz, I., García-Rodríguez, J. L., Buqué, X., Mestre, D., Luka, Z., Wagner, C., Alonso, C., Finnell, R. H., Lu, S. C., Martínez-Chantar, L. M., Aspichueta, P., & Mato, J. M. (2013). Excess S-adenosylmethionine reroutes phosphatidylethanolamine towards phosphatidylcholine and triglyceride synthesis. *Hepatology*, *58*(4), 1296-1305. https://doi.org/10.1002/hep.26399
Masoodi, M., Gastaldelli, A., Hyötyläinen, T., Arretxe, E., Alonso, C., Gaggini, M., Brosnan, J., Anstee, Q. M., Millet, O., & Ortiz, P. (2021). Metabolomics and lipidomics in NAFLD: biomarkers and non-invasive diagnostic tests. *Nature reviews Gastroenterology & hepatology*, *18*(12), 835-856.
Matic, I. (2018). The major contribution of the DNA damage-triggered reactive oxygen species production to cell death: implications for antimicrobial and

doi:10.6342/NTU202503955

cancer therapy. *Curr Genet*, *64*(3), 567-569. https://doi.org/10.1007/s00294-017-0787-3
Maximino, P., Horta, P. M., Santos, L. C. d., Oliveira, C. L. d., & Fisberg, M. (2015). Fatty acid intake and metabolic syndrome among overweight and obese women. *Revista Brasileira de Epidemiologia*, *18*, 930-942.
Mei, X., Xiang, W., Pan, W., Lin, Q., Jia, X., Zhang, X., Tang, X., Cheng, X., Weng, Y., Yang, K., & Lu, N. (2024). Plasmalogens Reversed Oxidative Stress and Inflammatory Response Exacerbated by Damage to Cell Membrane Properties in Acute Liver Injury. *J Agric Food Chem*, *72*(51), 28280-28293. https://doi.org/10.1021/acs.jafc.4c06929
Ming, Y. N., Zhang, J. Y., Wang, X. L., Li, C. M., Ma, S. C., Wang, Z. Y., Liu, X. L., Li, X. B., & Mao, Y. M. (2017). Liquid chromatography mass spectrometry-based profiling of phosphatidylcholine and phosphatidylethanolamine in the plasma and liver of acetaminophen-induced liver injured mice. *Lipids Health Dis*, *16*(1), 153. https://doi.org/10.1186/s12944-017-0540-4
Norris, P. C., & Dennis, E. A. (2012). Omega-3 fatty acids cause dramatic changes in TLR4 and purinergic eicosanoid signaling. *Proceedings of the National Academy of Sciences*, *109*(22), 8517-8522.
OECD, H. (2021). Reconciling terminology of the universe of per-and polyfluoroalkyl substances: recommendations and practical guidance. In (Vol. 61, pp. 45): OECD Publishing Paris.
Olsen, G. W., Burris, J. M., Ehresman, D. J., Froehlich, J. W., Seacat, A. M., Butenhoff, J. L., & Zobel, L. R. (2007). Half-life of serum elimination of perfluorooctanesulfonate,perfluorohexanesulfonate, and perfluorooctanoate in retired fluorochemical production workers. *Environ Health Perspect*, *115*(9), 1298-1305. https://doi.org/10.1289/ehp.10009
Pizzurro, D. M., Seeley, M., Kerper, L. E., & Beck, B. D. (2019). Interspecies differences in perfluoroalkyl substances (PFAS) toxicokinetics and application to health-based criteria. *Regul Toxicol Pharmacol*, *106*, 239-250. https://doi.org/10.1016/j.yrtph.2019.05.008
Post, G. B., Gleason, J. A., & Cooper, K. R. (2017). Key scientific issues in developing drinking water guidelines for perfluoroalkyl acids: Contaminants of emerging concern. *PLoS Biol*, *15*(12), e2002855. https://doi.org/10.1371/journal.pbio.2002855
Prentki, M., & Madiraju, S. R. M. (2008). Glycerolipid Metabolism and Signaling in Health and Disease. *Endocrine Reviews*, *29*(6), 647-676. https://doi.org/10.1210/er.2008-0007
Qin, Y., Gu, T., Ling, J., Luo, J., Zhao, J., Hu, B., Hua, L., Wan, C., & Jiang, S. (2022). PFOS facilitates liver inflammation and steatosis: An involvement of NLRP3 inflammasome-mediated hepatocyte pyroptosis. *J Appl Toxicol*, *42*(5), 806-817. https://doi.org/10.1002/jat.4258
Reiner, J. L., & Place, B. J. (2015). Perfluorinated alkyl acids in wildlife. *Toxicological Effects of Perfluoroalkyl and Polyfluoroalkyl Substances*, 127-150.
Riss, T. L., Moravec, R. A., Niles, A. L., Duellman, S., Benink, H. A., Worzella, T. J., & Minor, L. (2016). Cell viability assays. *Assay guidance manual [Internet]*.
Roth, K., Yang, Z., Agarwal, M., Liu, W., Peng, Z., Long, Z., Birbeck, J., Westrick, J., Liu, W., & Petriello, M. C. (2021). Exposure to a mixture of legacy, alternative, and replacement per- and polyfluoroalkyl substances (PFAS) results in sex-dependent modulation of cholesterol metabolism and liver injury. *Environ Int*, *157*, 106843. https://doi.org/10.1016/j.envint.2021.106843
Saher, G., Brügger, B., Lappe-Siefke, C., Möbius, W., Tozawa, R.-i., Wehr, M. C., Wieland, F., Ishibashi, S., & Nave, K.-A. (2005). High cholesterol level is essential for myelin membrane growth. *Nature neuroscience*, *8*(4), 468-475.
Sala, A., Proschak, E., Steinhilber, D., & Rovati, G. E. (2018). Two-pronged approach to anti-inflammatory therapy through the modulation of the arachidonic acid cascade. *Biochem Pharmacol*, *158*, 161-173. https://doi.org/10.1016/j.bcp.2018.10.007

doi:10.6342/NTU202503955

Salihovic, S., Stubleski, J., Karrman, A., Larsson, A., Fall, T., Lind, L., & Lind, P. M. (2018). Changes in markers of liver function in relation to changes in perfluoroalkyl substances - A longitudinal study. *Environ Int*, *117*, 196-203. https://doi.org/10.1016/j.envint.2018.04.052

Schmid, R., Heuckeroth, S., Korf, A., Smirnov, A., Myers, O., Dyrlund, T. S., Bushuiev, R., Murray, K. J., Hoffmann, N., Lu, M., Sarvepalli, A., Zhang, Z., Fleischauer, M., Duhrkop, K., Wesner, M., Hoogstra, S. J., Rudt, E., Mokshyna, O., Brungs, C.,…Pluskal, T. (2023). Integrative analysis of multimodal mass spectrometry data in MZmine 3. *Nat Biotechnol*, *41*(4), 447-449. https://doi.org/10.1038/s41587-023-01690-2

Serhan, C. N. (2014). Pro-resolving lipid mediators are leads for resolution physiology. *Nature*, *510*(7503), 92-101.

Shankar, A., Xiao, J., & Ducatman, A. (2011). Perfluoroalkyl chemicals and chronic kidney disease in US adults. *Am J Epidemiol*, *174*(8), 893-900. https://doi.org/10.1093/aje/kwr171

Stratakis, N., D, V. C., Jin, R., Margetaki, K., Valvi, D., Siskos, A. P., Maitre, L., Garcia, E., Varo, N., Zhao, Y., Roumeliotaki, T., Vafeiadi, M., Urquiza, J., Fernandez-Barres, S., Heude, B., Basagana, X., Casas, M., Fossati, S., Grazuleviciene, R.,…Chatzi, L. (2020). Prenatal Exposure to Perfluoroalkyl Substances Associated With Increased Susceptibility to Liver Injury in Children. *Hepatology*, *72*(5), 1758-1770. https://doi.org/10.1002/hep.31483

Sud, M., Fahy, E., Cotter, D., Brown, A., Dennis, E. A., Glass, C. K., Merrill Jr, A. H., Murphy, R. C., Raetz, C. R., & Russell, D. W. (2007). Lmsd: Lipid maps structure database. *Nucleic acids research*, *35*(suppl_1), D527-D532.

Svegliati-Baroni, G., Pierantonelli, I., Torquato, P., Marinelli, R., Ferreri, C., Chatgilialoglu, C., Bartolini, D., & Galli, F. (2019). Lipidomic biomarkers and mechanisms of lipotoxicity in non-alcoholic fatty liver disease. *Free Radic Biol Med*, *144*, 293-309. https://doi.org/10.1016/j.freeradbiomed.2019.05.029

Tang, C. H., Tsao, P. N., Chen, C. Y., Shiao, M. S., Wang, W. H., & Lin, C. Y. (2011). Glycerophosphocholine molecular species profiling in the biological tissue using UPLC/MS/MS. *J Chromatogr B Analyt Technol Biomed Life Sci*, *879*(22), 2095-2106. https://doi.org/10.1016/j.jchromb.2011.05.044

van der Veen, J. N., Kennelly, J. P., Wan, S., Vance, J. E., Vance, D. E., & Jacobs, R. L. (2017). The critical role of phosphatidylcholine and phosphatidylethanolamine metabolism in health and disease. *Biochim Biophys Acta Biomembr*, *1859*(9 Pt B), 1558-1572. https://doi.org/10.1016/j.bbamem.2017.04.006

Vance, D. E. (2014). Phospholipid methylation in mammals: from biochemistry to physiological function. *Biochim Biophys Acta*, *1838*(6), 1477-1487. https://doi.org/10.1016/j.bbamem.2013.10.018

Villas-Boas, S. G., Nielsen, J., Smedsgaard, J., Hansen, M. A., & Roessner-Tunali, U. (2007). *Metabolome analysis: an introduction*. John Wiley & Sons.

Wan, H., Zhao, Y., Wei, X., Hui, K., Giesy, J., & Wong, C. K. (2012). PFOS-induced hepatic steatosis, the mechanistic actions on β-oxidation and lipid transport. *Biochimica et Biophysica Acta (BBA)-General Subjects*, *1820*(7), 1092-1101.

Wang, J., He, W., Tsai, P. J., Chen, P. H., Ye, M., Guo, J., & Su, Z. (2020). Mutual interaction between endoplasmic reticulum and mitochondria in nonalcoholic fatty liver disease. *Lipids Health Dis*, *19*(1), 72. https://doi.org/10.1186/s12944-020-01210-0

Wang, J., Wang, C., & Han, X. (2019). Tutorial on lipidomics. *Anal Chim Acta*, *1061*, 28-41. https://doi.org/10.1016/j.aca.2019.01.043

Wang, L. Q., Liu, T., Yang, S., Sun, L., Zhao, Z. Y., Li, L. Y., She, Y. C., Zheng, Y. Y., Ye, X. Y., Bao, Q., Dong, G. H., Li, C. W., & Cui, J. (2021). Perfluoroalkyl substance pollutants activate the innate immune system through the AIM2 inflammasome. *Nat Commun*, *12*(1), 2915. https://doi.org/10.1038/s41467-021-23201-0

doi:10.6342/NTU202503955

Wee, S. Y., & Aris, A. Z. (2023). Environmental impacts, exposure pathways, and health effects of PFOA and PFOS. *Ecotoxicol Environ Saf*, *267*, 115663. https://doi.org/10.1016/j.ecoenv.2023.115663

Wilkening, S., Stahl, F., & Bader, A. (2003). Comparison of primary human hepatocytes and hepatoma cell line Hepg2 with regard to their biotransformation properties. *Drug Metab Dispos*, *31*(8), 1035-1042. https://doi.org/10.1124/dmd.31.8.1035

Yao, Z. M., & Vance, D. E. (1988). The active synthesis of phosphatidylcholine is required for very low density lipoprotein secretion from rat hepatocytes. *Journal of Biological Chemistry*, *263*(6), 2998-3004. https://doi.org/10.1016/s0021-9258(18)69166-5

Yen, T. H., Lee, S. H., Tang, C. H., Liang, H. J., & Lin, C. Y. (2024). Lipid responses to perfluorooctane sulfonate exposure for multiple rat organs. *Ecotoxicol Environ Saf*, *277*, 116368. https://doi.org/10.1016/j.ecoenv.2024.116368

Zhang, L., Krishnan, P., Ehresman, D. J., Smith, P. B., Dutta, M., Bagley, B. D., Chang, S. C., Butenhoff, J. L., Patterson, A. D., & Peters, J. M. (2016). Editor's Highlight: Perfluorooctane Sulfonate-Choline Ion Pair Formation: A Potential Mechanism Modulating Hepatic Steatosis and Oxidative Stress in Mice. *Toxicol Sci*, *153*(1), 186-197. https://doi.org/10.1093/toxsci/kfw120

Zhu, L., Yang, X., Feng, J., Mao, J., Zhang, Q., He, M., Mi, Y., Mei, Y., Jin, G., & Zhang, H. (2022). CYP2E1 plays a suppressive role in hepatocellular carcinoma by regulating Wnt/Dvl2/beta-catenin signaling. *J Transl Med*, *20*(1), 194. https://doi.org/10.1186/s12967-022-03396-6

doi:10.6342/NTU202503955

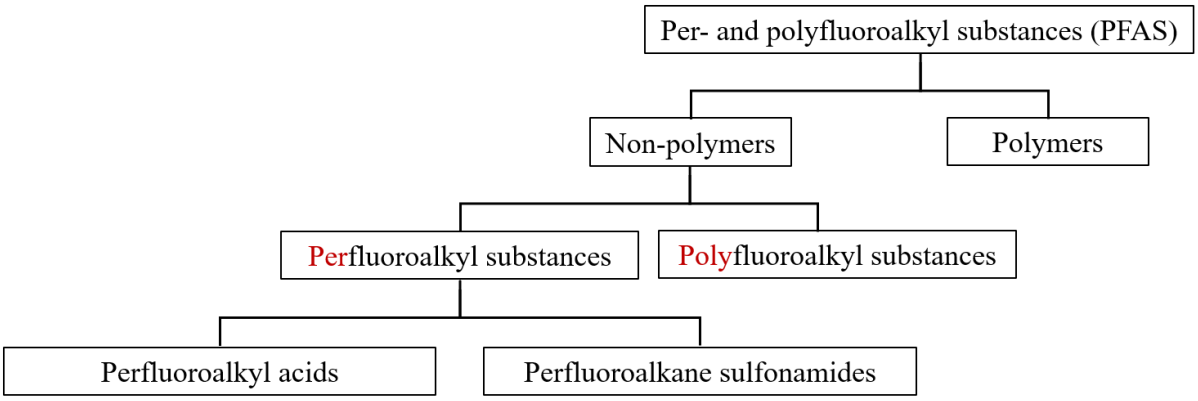

Figure 1 Structural classification framework of PFAS

doi:10.6342/NTU202503955

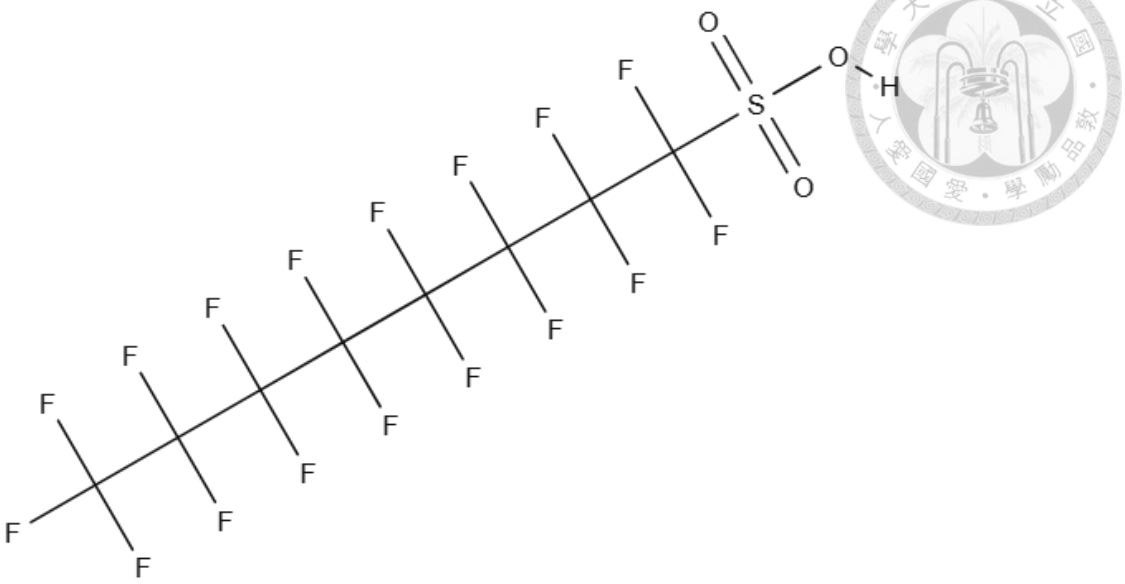

Figure 2 The structure of perfluorooctanesulfonic acid (PFOS)

doi:10.6342/NTU202503955

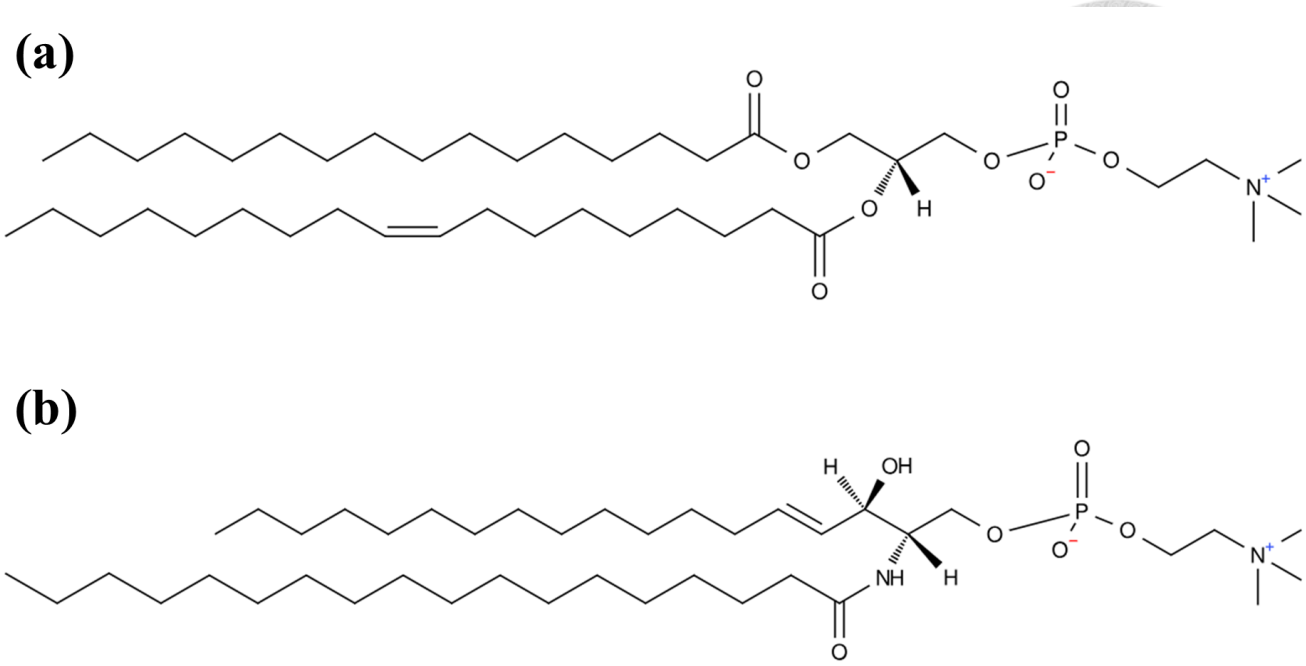

Figure 3 The representative structure of phosphorylcholine-containing lipids (a) phosphatidylcholine, (b) sphingomyelin.

doi:10.6342/NTU202503955

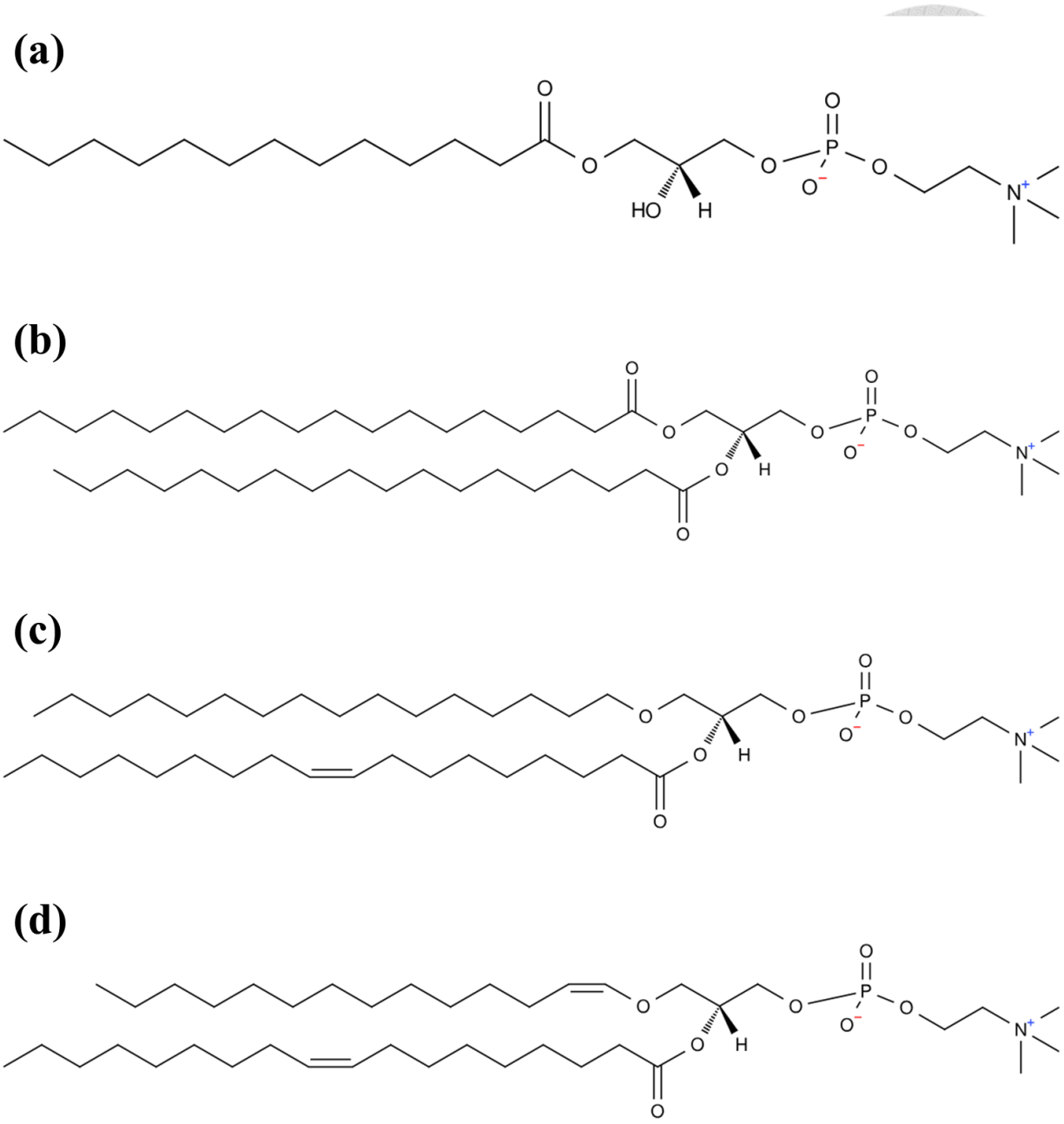

Figure 4 The representative structure of different species of the phosphatidylcholines (a) lyso-phosphatidylcholines, (b) diacyl-phosphatidylcholines, (c) O-alkyl-acyl- phosphatidylcholines, and (d) O-alkenyl-acyl- phosphatidylcholines.

doi:10.6342/NTU202503955

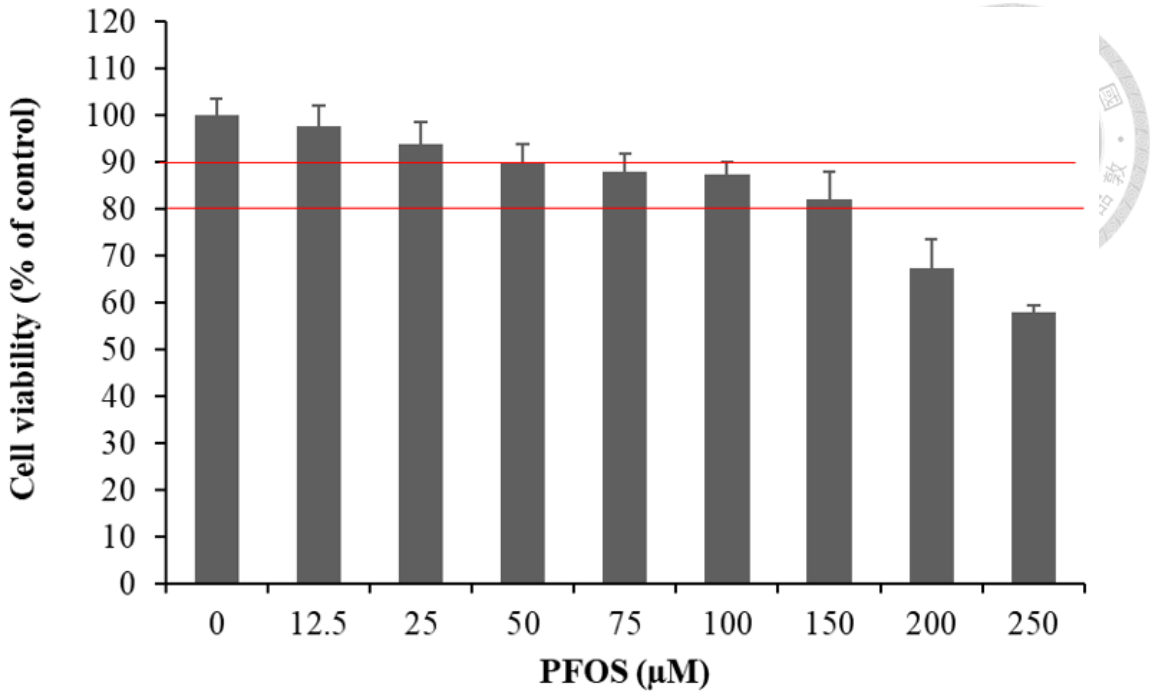

Figure 5 The cell viability of HepG2 cells treated with various doses of PFOS.
The results are presented as the mean ± standard deviation (SD).
The red line at the top indicates 90% cell viability, while the red line at the bottom indicates 80% cell viability.

doi:10.6342/NTU202503955

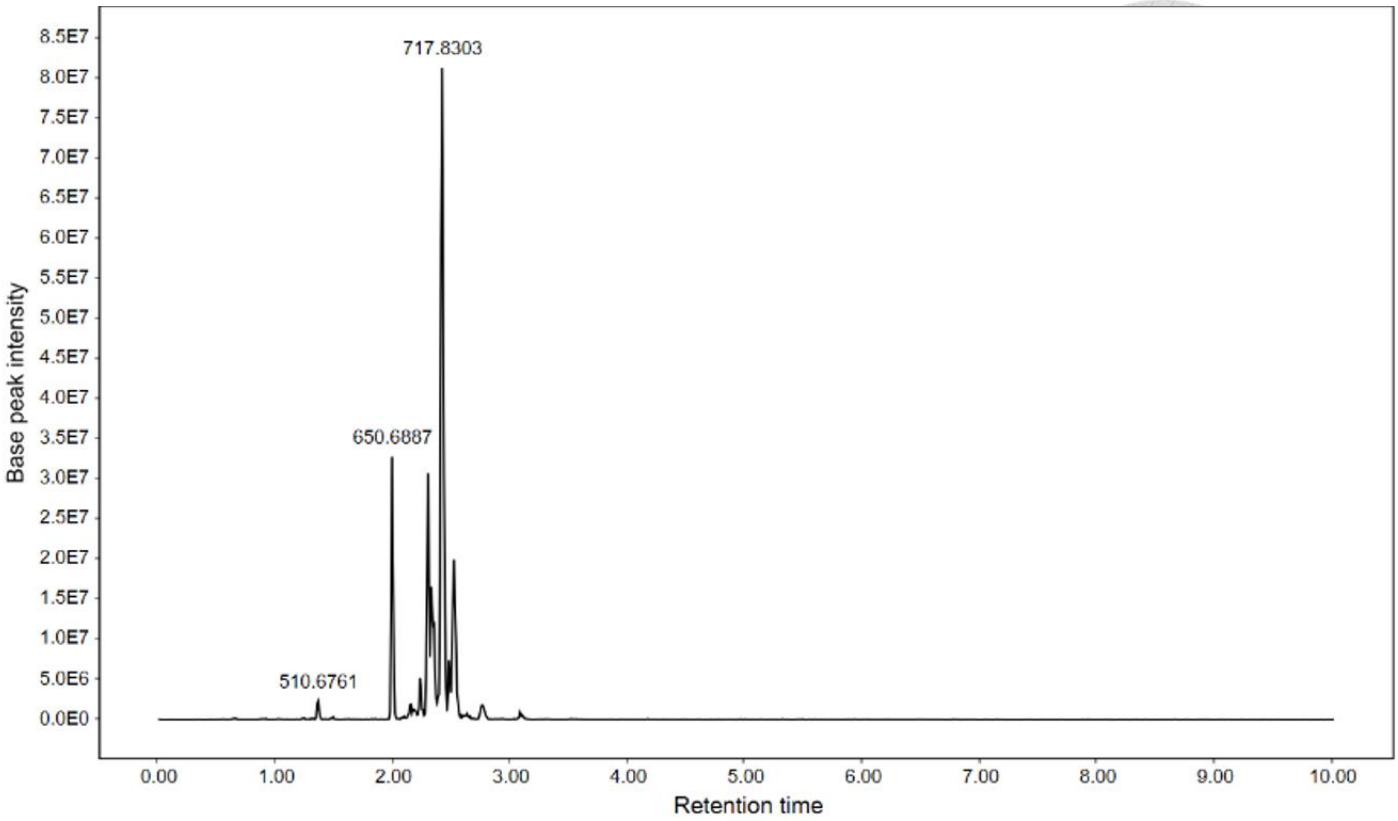

Figure 6 Total ion chromatogram (TIC) of a QC sample from the analysis of HepG2 cells treated with various concentrations of PFOS.

The mass-to-charge ratios of 510.6761, 650.6887, and 717.8303 correspond to the lipid standards PC(17:0/0:0), PC(13:0/13:0), and SM(d18:1/17:0), respectively standards PC(17:0/0:0), PC(13:0/13:0), and SM(d18:1/17:0), respectively.

doi:10.6342/NTU202503955

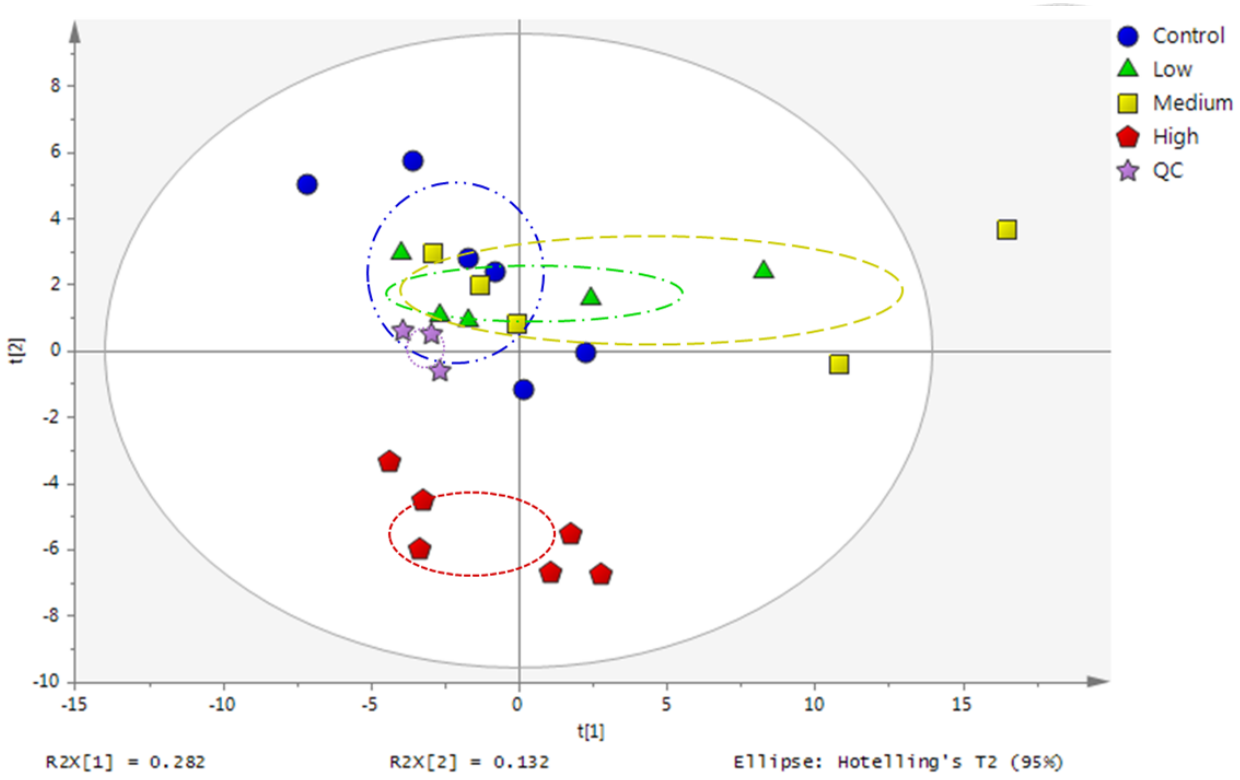

Figure 7 The PCA score plot from the analysis of spectral data of HepG2 cells treated with various doses of PFOS.

Symbol designation: Control group [●], [—··—]; Low dose group (1/10 IC_{10}) [▲], [—·—]; Medium dose (IC_{10}) [■], [— —] ; High dose group (IC_{20}) [⬟], [– –]; Quality control samples (QC) [★], [··].

Outer ellipse: Hotelling's T2 with 95% confidence interval; Five inner dash/dot ellipses: Calculated from the mean ± the standard deviation in each group.

The control, low dose, medium dose, and high dose groups correspond to PFOS exposure concentrations of 0, 5, 50, and 150 μM, respectively.

doi:10.6342/NTU202503955

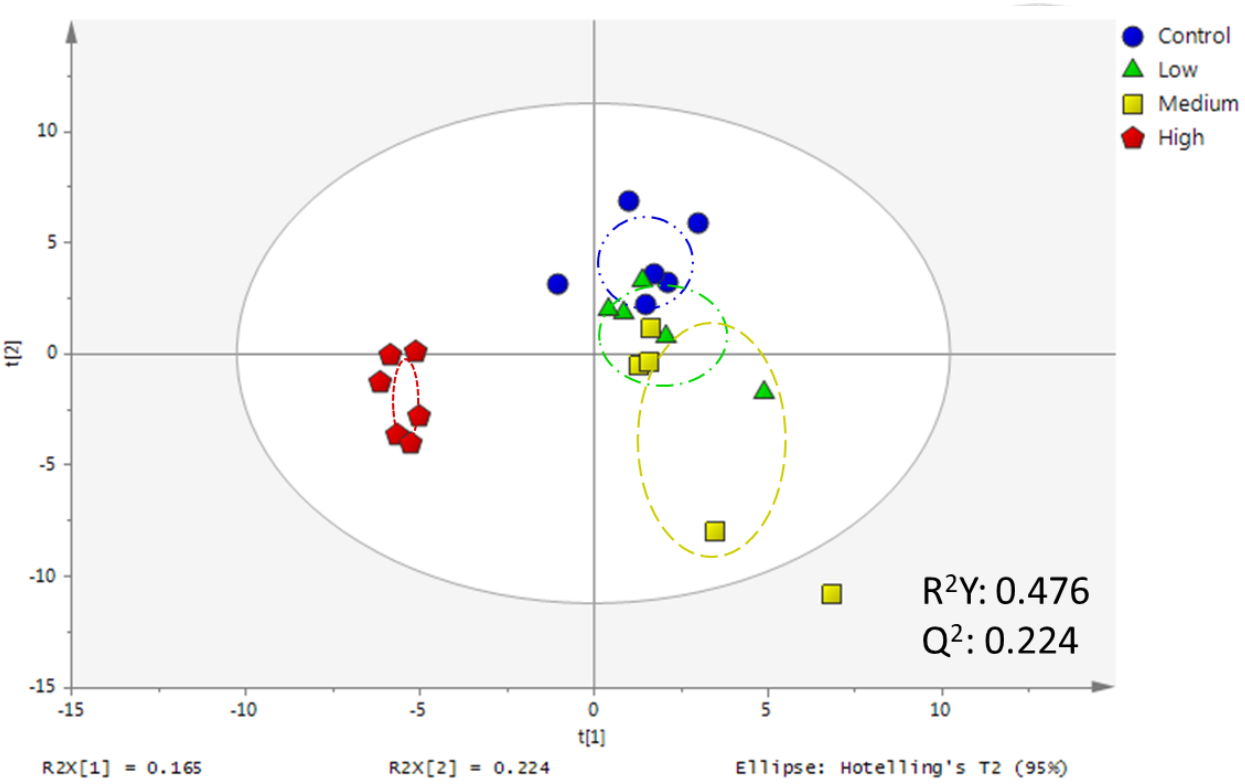

Figure 8 The PLS-DA score plot from the analysis of spectral data of HepG2 cells treated with various doses of PFOS.

Symbol designation: Control group [●], [—·—]; Low dose group (1/10 IC_{10}) [▲], [—·—]; Medium dose (IC_{10}) [■], [— —]; High dose group (IC_{20}) [⬟], [– –].

Outer ellipse: Hotelling's T2 with 95% confidence interval; Four inner dash/dot ellipses: Calculated from the mean ± the standard deviation in each group.

The control, low dose, medium dose, and high dose groups correspond to PFOS exposure concentrations of 0, 5, 50, and 150 μM, respectively.

doi:10.6342/NTU202503955

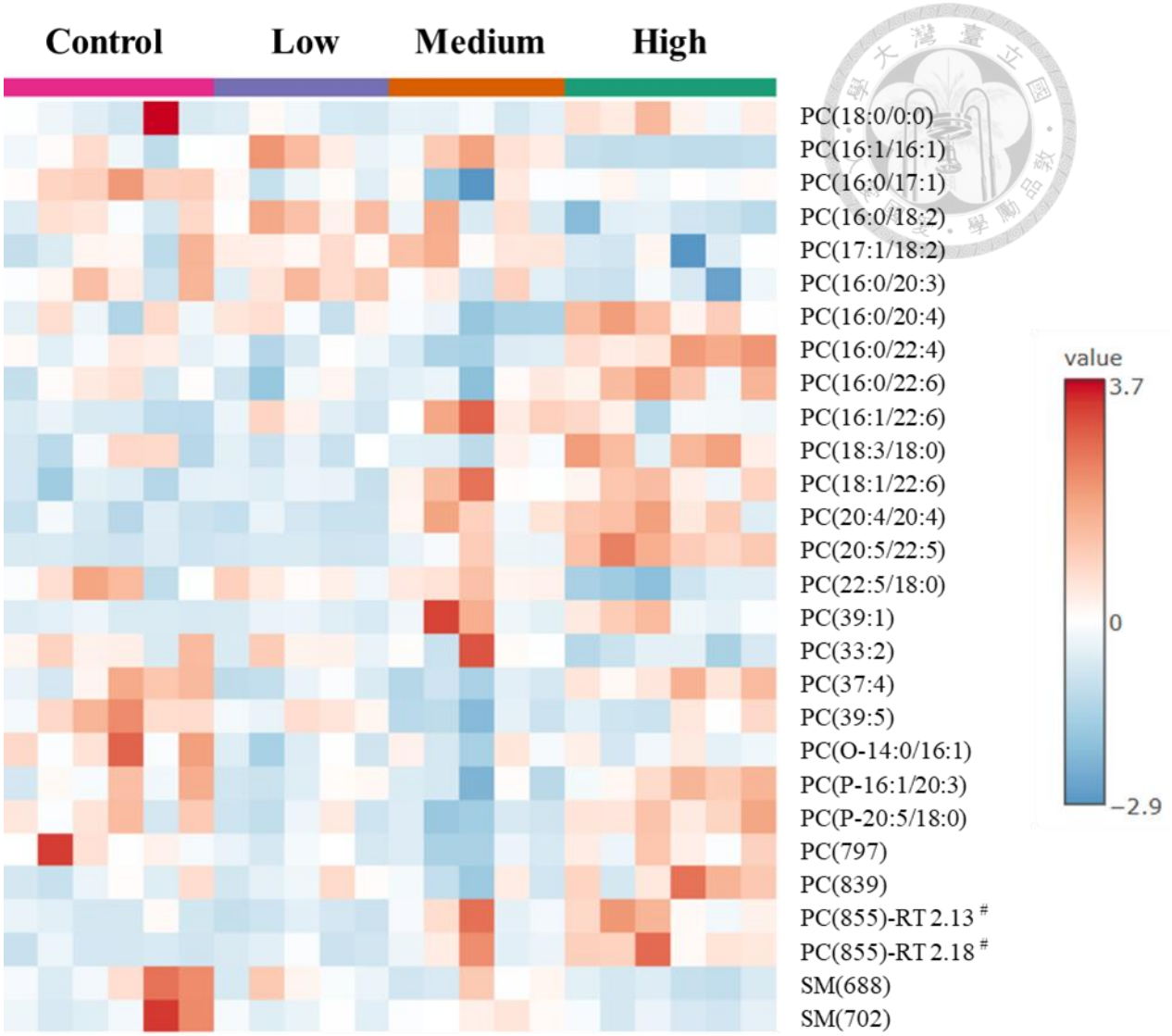

Figure 9 Heatmap of significantly altered lipids in HepG2 cells treated with various doses of PFOS. Statistical significance was identified by Kruskal–Wallis test.

#: Mass to charge ratios of lipid isomers were consistent across various retention times: 2.13 and 2.18 min for PC (855)

PC: phosphatidylcholine, SM: sphingomyelin

doi:10.6342/NTU202503955

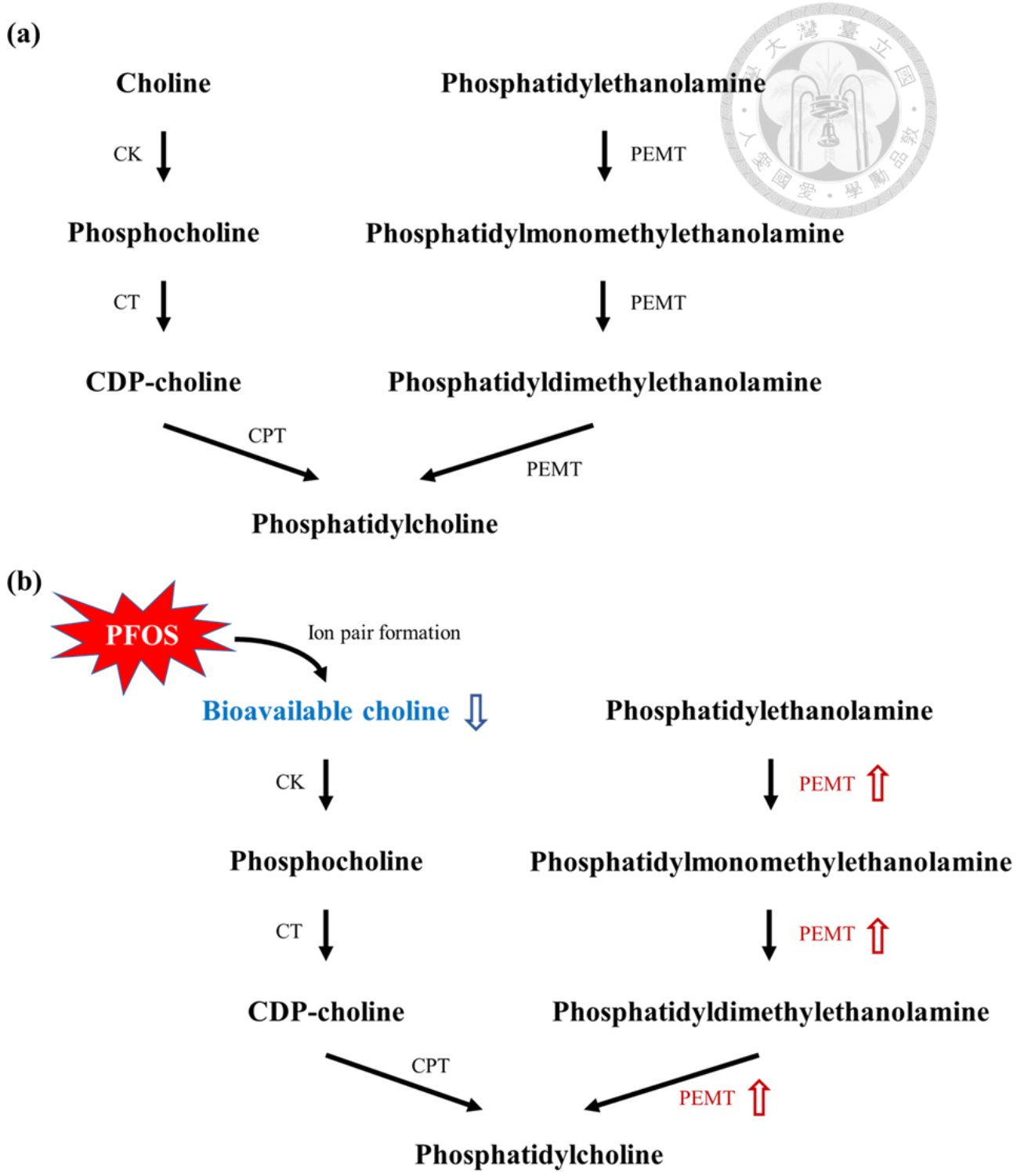

Figure 10 Overview of hepatic phosphatidylcholine synthesis via the CDP-choline and PEMT pathways under (a) normal conditions and (b) PFOS exposure.
CK: choline kinase, CT: phosphocholine cytidylyltransferase, CPT: 1,2-diacylglycerol choline phosphotransferase, PEMT: phosphatidylethanolamine N-methyltransferase.

doi:10.6342/NTU202503955

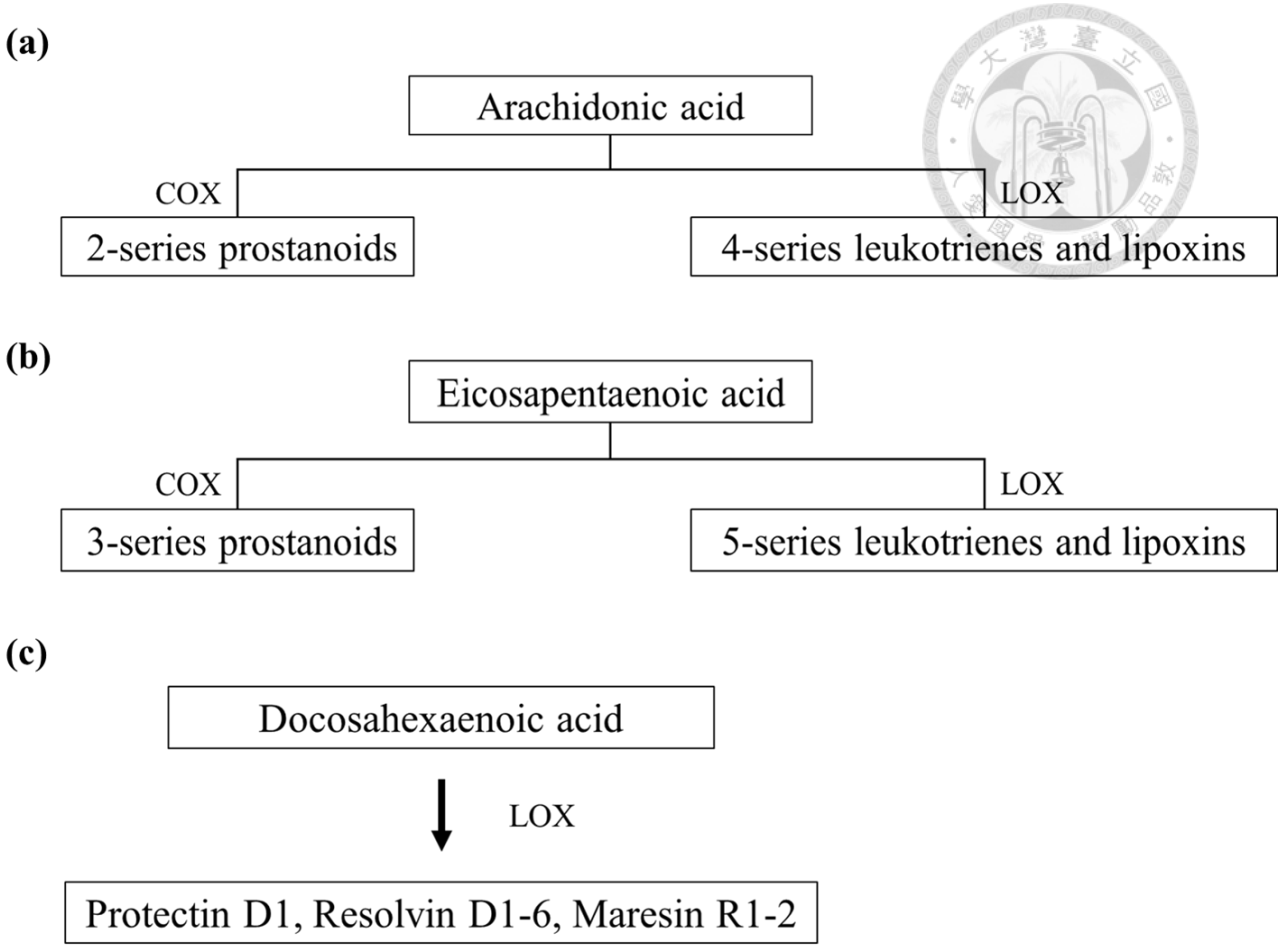

Figure 11 Overview of essential fatty acid conversion via cyclooxygenase (COX) and lipoxygenase (LOX) pathways.
(a) arachidonic acid (AA), (b) eicosapentaenoic acid (EPA), and (c) docosahexaenoic acid (DHA)

doi:10.6342/NTU202503955

Table 1 Comparison between human liver cell lines

	HepG2 Cells	**HepaRG Cells**	**Primary Hepatocytes**
Cell origin	Human hepatocellular carcinoma	Human hepatocarcinoma (can differentiate into hepatocyte-like and biliary cells)	Human liver tissue
Differentiation requirement	None	Require differentiation	No
Applications	Cytotoxicity screening, high-throughput toxicology, lipidomics	Drug metabolism studies, hepatotoxicity mechanisms, lipid metabolism research	Gold standard for xenobiotic metabolism, transporter studies
Major advantages	Easy to culture, fast growth, high reproducibility, cost-effective	High metabolic capacity, better mimic of human liver function	Full metabolic function, most physiologically relevant
Major limitations	Low CYP enzyme activity, limited liver-specific functions, cancer-derived	Long differentiation time, more complex culture conditions, higher cost	Donor variability, limited availability, short-term culture viability

doi:10.6342/NTU202503955

Table 2 A list of stable lipid features in pooled quality control sample of PFOS-treated HepG2 cells

Lipid category	Detected m/z	Detected RT (min)	Compound name
LPC	522.5	1.23	PC(0:0/18:1)
	524.5	1.43	PC(18:0/0:0)
DPC	678.6	2.15	PC(14:0/14:0)
	734.6	2.48	PC(16:0/16:0)
	748.7	2.60	PC(17:0/16:0)
	762.6	2.77	PC(18:0/16:0)
	790.3	3.08	PC(18:0/18:0)
	732.6	2.39	PC(16:0/16:1)
	732.6	2.33	PC(16:1/16:0)
	730.6	2.18	PC(16:1/16:1)
	746.6	2.42	PC(16:0/17:1)
	760.6	2.52	PC(16:0/18:1)
	774.4	2.64	PC(17:0/18:1)
	788.7	2.77	PC(18:0/18:1)
	758.6	2.34	PC(16:0/18:2)
	756.6	2.20	PC(16:1/18:2)
	772.6	2.42	PC(17:0/18:2)
	770.4	2.28	PC(17:1/18:2)
	786.6	2.53	PC(18:0/18:2)
	782.6	2.22	PC(18:2/18:2)
	800.7	2.63	PC(19:0/18:2)
	784.6	2.35	PC(16:0/20:3)
	782.6	2.30	PC(16:0/20:4)
	780.6	2.16	PC(16:0/20:5)
	778.4	2.09	PC(16:1/20:5)
	810.6	2.48	PC(16:0/22:4)
	808.6	2.30	PC(16:0/22:5)+PC(18:1/20:4)
	806.6	2.23	PC(16:0/22:6)
	804.5	2.10	PC(16:1/22:6)
	784.5	2.39	PC(18:3/18:0)
	812.4	2.60	PC(18:0/20:3)
	806.7	2.18	PC(18:2/20:4)
	834.7	2.35	PC(18:0/22:6)
	838.5	2.62	PC(18:0/22:4)
	836.6	2.47	PC(18:0/22:5)
	832.6	2.23	PC(18:1/22:6)
	824.7	2.59	PC(19:0/20:4)
	838.7	2.71	PC(20:0/20:4)
	830.4	2.13	PC(20:4/20:4)
	854.6	2.08	PC(20:5/22:5)
	820.5	2.24	PC(22:6/17:0)
	836.6	2.42	PC(22:5/18:0)

doi:10.6342/NTU202503955

Table 2 (continued) List of stable lipid features in pooled quality control sample of PFOS-treated HepG2 cells

Lipid category	Detected m/z	Detected RT (min)	Compound name
DPC	858.6	2.23	PC(22:5/20:3)
	744.6	2.26	PC(33:2)
	754.6	2.14	PC(34:4)
	768.6	2.22	PC(35:4)
	796.6	2.39	PC(37:4)
	818.5	2.46	PC(38:0)
	828.3	2.04	PC(39:1)
	822.6	2.39	PC(39:5)
	834.6	2.29	PC(40:6)
O-PC	692.6	2.44	PC(O-16:0/14:0)
	690.6	2.39	PC(O-14:0/16:1)
	744.7	2.46	PC(O-16:0/18:2)
P-PC	718.5	2.61	PC(P-16:0/16:0)
	800.3	2.94	PC(P-21:1/17:0)
	798.5	2.44	PC(P-20:0/18:2)
	768.6	2.41	PC(P-16:0/20:3)
	766.6	2.36	PC(P-16:1/20:3)
	790.6	2.29	PC(P-16:1/22:5)
	792.6	2.36	PC(P-20:5/18:0)
	794.6	2.56	PC(P-38:4)
Unidentified PC	706.7	2.55	PC(705)
	734.6	2.52	PC(733)
	746.4	2.90	PC(745)
	748.6	2.63	PC(747)
	752.6	2.27	PC(751)
	754.6	2.31	PC(753)
	780.5	2.43	PC(779)
	784.7	2.44	PC(783)
	788.5	2.25	PC(787)
	796.7	2.31	PC(795)
	798.7	2.48	PC(797)
	822.8	2.34	PC(821)
	830.7	2.42	PC(829)
	834.6	2.40	PC(833)
	836.7	2.55	PC(835)
	840.6	2.30	PC(839)
	846.8	2.76	PC(845)
	856.7	2.13	PC(855)-RT 2.13[#]
	856.6	2.18	PC(855)-RT 2.18[#]
	862.7	2.43	PC(861)
	866.6	2.30	PC(865)
	882.5	2.17	PC(881)
	884.5	2.24	PC(883)

doi:10.6342/NTU202503955

Table 2 (continued) List of stable lipid features in pooled quality control sample of PFOS-treated HepG2 cells

Lipid category	Detected m/z	Detected RT (min)	Compound name
Unidentified SM	647.7	1.96	SM(646)
	675.6	2.14	SM(674)
	689.7	2.23	SM(688)
	701.6	2.15	SM(700)
	703.6	2.32	SM(702)
	715.5	2.24	SM(714)
	717.8	2.26	SM(716)
	731.7	2.54	SM(730)
	757.7	2.54	SM(756)
	773.2	2.50	SM(772)
	789.9	2.25	SM(788)
	835.5	2.34	SM(834)

[#]: Mass to charge ratios of lipid isomers were consistent across various retention times: 2.13 and 2.18 min for PC (855).

LPC: lyso-phosphatidylcholine; DPC: diacyl-phosphatidylcholine; O-PC: O-alkyl-acyl- phosphatidylcholine; P-PC: O-alkenyl-acyl- phosphatidylcholine; SM: sphingomyelin; RT: retention time

doi:10.6342/NTU202503955

Table 3 Significantly changed lipids in PFOS treated HepG2 cells using Kruskal-Wallis test

Lipids	Fold change			Kruskal-Wallis test (p-value)
	Low / Control	Medium / Control	High / Control	
PC(18:0/0:0)	0.63	0.94	2.90 *	0.0359
PC(16:1/16:1)	1.26	1.40	0.50	0.0053
PC(16:0/17:1)	0.73 **	0.79 *	0.79 *	0.0193
PC(16:0/18:2)	1.22	0.89	0.77 *	0.0121
PC(17:1/18:2)	1.19	1.26	0.85	0.0294
PC(16:0/20:3)	1.13	0.90	0.69 *	0.0400
PC(16:0/20:4)	1.12	0.74	1.33 *	0.0075
PC(16:0/22:4)	0.87	0.65 *	1.67	0.0008
PC(16:0/22:6)	0.83	0.90	1.29	0.0403
PC(16:1/22:6)	1.36	2.85 ***	1.55	0.0083
PC(18:3/18:0)	0.97	0.93	2.96 *	0.0401
PC(18:1/22:6)	1.17	1.71 **	1.99 **	0.0009
PC(20:4/20:4)	0.75	3.90 *	5.01 **	0.0024
PC(20:5/22:5)	0.84	2.73 *	9.50 ***	0.0006
PC(22:5/18:0)	1.00	1.06	0.38 **	0.0101
PC(39:1)	1.53	3.57	6.90 **	0.0062
PC(33:2)	0.98	0.89	0.49 **	0.0235
PC(37:4)	0.46	0.38 **	0.93	0.0048
PC(39:5)	0.81	0.38 ***	0.67 *	0.0034
PC(O-14:0/16:1)	0.46 **	0.64 *	0.60	0.0261
PC(P-16:1/20:3)	0.77	0.71 *	1.36	0.0194
PC(P-20:5/18:0)	0.46 *	0.48 *	1.07	0.0041
PC(797)	0.71 *	0.52 **	1.12	0.0032
PC(839)	1.14	0.77	2.03 *	0.0473
PC(855)-RT 2.13 #	0.63	1.72	2.80 *	0.0017
PC(855)-RT 2.18 #	1.31	2.48 *	6.08 ***	0.0021
SM(688)	0.86	0.89	0.63 **	0.0454
SM(702)	0.96	1.12	0.90	0.0350

#: Mass to charge ratios of lipid isomers were consistent across various retention times: 2.13 and 2.18 min for PC (855).

PC: phosphatidylcholine, SM: sphingomyelin

Significant p values are noted by * ($p < 0.05$), **($p < 0.01$), ***($p < 0.001$) in Dunn's test

doi:10.6342/NTU202503955